

*Author reply (AR)*

Dear Marcel van der Meer,

*Thanks for providing us the opportunity to revise our manuscript further. We would also like to thank the two reviewers and you for your valuable comments and recommendations to improve our manuscript. We carefully revised and modified the document following your latest suggestions and comments. In addition, we made extra modifications to the text to improve the clarity and focus of the whole manuscript.*

*Please find the detailed response (AR, blue italic font) to your comments and the changes made to the manuscript (ACMS, blue bold font). The precise line in the previous and in the revised version of the manuscript where each change was made is provided as well. Additionally, we provide a new version with tracked changes (this file), and a pdf version of the new manuscript (separate file). We believe that the revised version satisfactorily addresses your questions and concerns and hope that the manuscript is now acceptable to BG. Should you have any additional requests or questions, please do not hesitate to contact me.*

*We are looking forward to hearing from you.*

*Sincerely,*

*Carolina Cisternas-Novoa*

BG-2018-360 decision

Editor comment (EC): Dear Carolina Cisternas-Novoa,

First of all I would like to thank both reviewers again for their insightful reviews and you for your better organized comments. I think the manuscript has improved significantly, but do still have some smaller and perhaps bigger issues. I guess one of the more major comments has to do with your MnOx-like particles, they are MnOx-like up until page 31 and then they become MnOx? Looking at your M&M section, I am not entirely clear what they are. If the method you describe for measurement of these particles is known to target MnOx particles I would expect one or more references indicating this. If not, than how do you know what these particles are? If they do contain MnOx, please indicate how you know, is MnOx-like the best name for them? MnOx containing might be better?

What is CSP? I know what it stands for, but what is it? Proteins or particle containing relatively large amounts of proteins? Is CSP correlated to DI?

*Author Reply (AR):*

**1. *Regarding terminology discrepancy MnOx-like particles vs. MnOx containing particles.***

*MnOx containing particles have been previously identified in the chemocline of Gotland Basin (GB, Dellwig et al., 2010; Dellwig et al., 2018; Glockzin et al., 2014; Neretin et al., 2003) and Landsort Deep (LD, Glockzin et al., 2014; Dellwig et al., 2010). The maximum abundance of those particles, coincide with the maximum concentration of particulate Mn and is located at the depth were O<sub>2</sub> concentration is ≤ 20 μM and above measurable H<sub>2</sub>S (Neretin et al., 2003).*

*Commonly MnOx containing particles are identified based on their morphologies, size and their elemental composition which is confirmed using a scanning electron microscopy (SEM) and energy dispersive x-ray microanalysis (EDX) (Neretin et al., 2003; Glockzin et al., 2014; Dellwig et al., 2010, 2018)*

*In our study, we did not measure the elemental composition of the particles. Thus, we identified them as "MnOx-like particles" based on similar morphology, size, and association with organic matter (OM) as MnOx containing particles previously reported for the Baltic Sea (e.g., Neretin et al., 2003 and Glockzin et al., 2014). The vertical distribution of our MnOx-like particles in the water column and sediment traps showed maximum concentration at the GB when the O<sub>2</sub> concentration was 40 μM or lower, and no particles were visualized in the filters after the H<sub>2</sub>S was measurable in the LD.*

*Moreover, the vertical profile of MnOx-like particles in the GB in our study coincides with the dynamics of MnOx containing particles following the 2014-2015 MBI described by Dellwing et al. (2018). Their results showed a remarkable deposition of MnOx containing particles in the water column profiles and in sediment traps material collected at 186 m. In addition, the maximum concentration of particulate Mn was measured in the water column at 128 and 233 m in July 2015, which agreed with the vertical profile of Mn-like particles in the water column and in the sediment trap material that we found in this study.*

*The evidence mentioned above, strongly suggests that the particles observed and quantified in our study correspond to the previously reported MnOx containing particles. However, since we did not perform a chemical analysis to ensure their exact elemental composition, and instead define those particles based in their morphology, size and OM association we call them "MnOx-like particles." We quantified and sized them using particle recognition on filters and imaging processing as described in the methods section and similar to the method used by Neretin et al. (2003).*

*We carefully checked the text to ensure the use the term "MnOx-like particles" consistently when we refer to the particles identify and described in this study and differentiate them from previously reported MnOx containing particles.*

- **Author's changes in manuscript (ACMS):**

**We added a paragraph to the method section explaining how we identified and quantified MnOx-like particles L255-269:**

**"MnOx-containing particles have been commonly identified based on their morphology, size and elemental composition, confirmed by scanning electron microscopy (SEM) and energy dispersive x-ray microanalysis (EDX) (Neretin et al., 2003; Glockzin et al., 2014; Dellwig et al., 2010, 2018). In this study, we did not measure the elemental composition of the particles. Thus, we identified them as "MnOx-like particles" based on similar morphology, size, and association with organic matter (OM) as MnOx-containing particles previously described in the Baltic Sea (eg., Neretin et al., 2003 and Glockzin et al., 2014). The abundance and size of MnOx-like particles were determined using particle recognition on filters and imaging processing similar to the method used by Neretin et al. (2003) but without the chemical composition analysis of the particles. For the image analysis, we used the same images as for TEP and CSP analysis and modified image analysis procedure described above as follows: thirty images per filter (200x) were analyzed semi-automatically using ImageJ software. After RGB split, the blue channel pictures were used to quantify MnOx-like particles in the water column and sediment traps. In this manner, the MnOx-like particles were clearly visible with a negligible disruption from TEP or CSP stained blue."**

We added a paragraph explaining why the particles in our study, denominated “MnOx-like particles”, may correspond to the previously reported MnOx containing particles L611-617:

“The high flux of POC at GB coincided with the appearance of dark, star-shaped particles that we defined as MnOx-like particles, particularly evident at GB (Fig. 6a,b, and e), but also present in LD. Based on their morphology, size, and aggregation with OM, we propose that those particles correspond to MnOx-containing particles enriched in OM that have been previously described at GB (Neretin et al., 2003; Pohl et al., 2004; Glockzin et al., 2014; Dellwig et al., 2010, 2018) and LD (Glockzin et al., 2014; Dellwig et al., 2010)”

2. Regarding Coomassie stainable particles (CSP)

- *Limited understanding of CSP chemical composition.*

*CSP are a protein containing exopolymeric particles that are abundant and ubiquitous in aquatic systems. CSP are transparent, so in order to visualize them, they need first to be stain with Coomassie Brilliant Blue, a dye commonly used to stain proteins (Bradford, 1976).*

*Phytoplankton (diatoms and cyanobacteria) and heterotrophic bacteria are sources of CSP. Scarce studies had examining CSP properties and dynamics; it has been suggested that CSP are less sticky and more labile than TEP (Thornton, 2018), but there is no information about the amount of carbon and nitrogen that CSP contain or their specific composition regarding amino acids.*

*The limited information about the chemical composition of CSP constrains our understanding of the relationship between CSP and other biogeochemical relevant parameters such as the amino acid-based degradation index (DI). Theoretically, if CSP are enriched in labile proteins, we could expect a significant correlation with a DI that indicate fresher material (positive). Our results showed that there is not a significant relationship between TAA flux and CSP flux ( $r^2=0.2$ ,  $p=1$ ); but there was a significant positive relationship between CSP flux and DI ( $R^2=0.84$ ,  $P<0.005$ , data not shown). However, due to the lack of information on their exact chemical composition, this assumption would need to be explored further before establishing a relationship.*

*In this research, we studied CSP to investigate if they aggregate with particles similar to TEP do; our results showed that when MnOx-like particles are abundant in the water column, they aggregate not only with TEP but also with CSP (Figure 6).*

- **ACMS:**

We added a paragraph in the introduction indicating the significance of CSP for this study, L155-161: “Another type of less studied exopolymer particles are Coomassie stainable particles (CSP), they are protein-containing particles that stain with Coomassie brilliant blue (Long and Azam 1996). Little is known about the characteristics and dynamics of those particles in marine systems and their potential to form aggregates with MnOx had not been studied. Different to TEP, CSP have a limited role on the aggregation of diatoms (Prieto et al., 2002; Cisternas-Novoa et al., 2015), but seem to be important for the aggregation of cyanobacteria (Cisternas-Novoa et al., 2015)”

We change the starting sentence about TEP and CSP in the method section, L234-235 “Polysaccharide (TEP) and protein (CSP) exopolymer particles, from sediment

trap and water column samples were analyzed by microscopy according to Engel (2009).”

We add a sentence to the method section indicating the specific dyes that are used to studied TEP and CSP, L235-239 “Duplicate aliquots of 5 to 20 mL were filtered onto 0.4  $\mu$ m Nuclepore membrane filters (Whatmann) and stained with 1 mL of Alcian Blue solution, a dye that target acidic polysaccharides, for TEP or 1 mL of Coomassie brilliant blue solution, a dye commonly used to stain proteins (Bradford, 1976), for CSP.”

Minor comments:

Line 16: “Sinking particles are the main form in which photosynthetically fixed carbon is transported from the euphotic zone to the ocean interior, the so called biological pump (BCP)”. And of course you can discuss the Baltic being an ocean.

*AR: We modify this sentence.*

**ACMS: L18-19, this sentence was modified to “Particle sinking is a major form to transport photosynthetically fixed carbon below the euphotic zone via the biological carbon pump (BCP)”**

Line 22: GB, but not

*AR: We added a comma to this sentence*

**ACMS: L24, this sentence was modified to “GB, but not”**

Line 25: oxygenated by the inflow of relatively saline waters from the North Sea?

*AR: We modified this paragraph and include the editor recommendation*

**ACMS: L23-25, this sentence was modified to “The two basins showed different oxygen regimes resulting from the intrusion of oxygen-rich water from the North Sea that ventilated the water column below 140 m in GB, but not in LD.”**

Line 28: POC has not been defined. Abbreviations and acronyms are typically defined the first time you use them in the abstract and again in the main text. If you only use them once, just use the full name.

*AR: We defined POC in line 30, which is the first time that we used in the abstract and in text. All the abbreviations definitions were checked to make sure we defined them the first time that we used*

**ACMS: L32, this sentence was modified to: “particulate organic carbon (POC)”**

Line 48: We’re in the main text now so define BCP again.

Line 49: POC is defined, great, do the same in the abstract.

**ACMS: We define the followings abbreviations:**

**L35 (Abstract): chlorophyll a (Chl a)**

**L56 (main text): biological carbon pump (BCP)**

**L64: oxygen (O<sub>2</sub>)**

Line 53-54: What do these authors mean with “higher refractory nature of sinking particles in the OMZ?”

*AR: This mechanism refers to the sinking fluxes associated to lithogenic minerals and refractory terrestrial OM, currently this type of OM have been mostly study in oxic water column while its contribution to POC flux in OMZ remains largely unexplored (Keil et al., 2016; Van Mooy et al., 2002).*

**ACMS: L62-63, these sentences were modified to “the potentially high contribution of refractory terrestrial organic matter (OM) to the POC flux (Keil et al., 2016; Van Mooy et al., 2002)”**

Line 58-60: Didn’t you just give that information?

*AR: This paragraph aims to point out that most of the research on POC flux in OMZ has been done in the tropical ocean; thus, there is not sufficient knowledge about how low O<sub>2</sub> could affect POC flux in temperate-boreal continental shelf regimes such as the Baltic Sea.*

**ACMS: L67-71, the paragraph was modified to “Currently, the study of POC vertical flux in OMZ’s has been mostly focused on the tropical ocean (Cavan et al., 2017; Devol and Hartnett, 2001; Engel et al., 2017; Keil et al., 2016; Van Mooy et al., 2002); whereas, how low O<sub>2</sub> concentration would affect the composition and fate of sinking OM, and the efficiency of the BPC in oxygen-deficient zones of temperate-boreal regimes such as the Baltic deep basins had been less studied.”**

Line 70: Gotland Basin (GB)

*AR: We defined the GB abbreviation here and deleted it from the L92*

**ACMS: L81, this sentence was modified to “Gotland Basin (GB)”**

Line 73: Define OM or even POM

*AR: We defined POM in L78 (previously L73)*

**ACMS: L85, this sentence was modified to “particulate organic matter (POM)”**

Line 84: “... would be necessary the bottom water....”?

*AR: We modified this paragraph for clarity*

**ACMS: L94-97, this paragraph was modified to “However, since hypoxia occurred naturally in the Baltic Sea due to physical processes, mitigating eutrophication will only decrease the spatial extent and intensity of the O<sub>2</sub> deficiency in the deep basins.”**

Line 85: Gotland Basin, used before in line 70, define GB in line 70.

*AR: We defined GB in L75 (previously L70)*

**ACMS: L97, this sentence was modified to “GB (248 m) and Landsort Deep (LD, 460 m)”**

Line 87: just Kattegat should do I think.

*AR: We deleted "Strait"*

**ACMS: L99, this sentence was modified to "limited water exchange with the North Sea through the Kattegat"**

Line 98: GB, it has been defined now.

*AR: We replaced "Gotland Basin" by "GB" in L105*

**ACMS: L112, this sentence was modified to "the MBI had reached GB"**

Line 105: "Water column stratification..."

*AR: This sentence was deleted because the paragraph was modified for clarity.*

Line 108: Does that redoxcline still exists during/after the MB?

*AR: The 2014/2015 MBI altered the water column profiles in the GB from March to February 2015. The oxygenated waters reached GB in March 2015, and deep water anoxia started to be re-established in July 2015, a subsequent minor inflow event re-oxygenated the deep waters of GB in February 2016. We reorganize the entire paragraph to clearly separate the "regular hypoxic conditions" from the scenario generated by the MBI.*

**ACMS: L97-117, the paragraph was modified to: "GB (248 m) and Landsort Deep (LD, 460 m) are the deepest basins of the Baltic Sea. They exhibit permanent bottom-water hypoxia (Conley et al. 2002), caused by a combination of limited water exchange with the North Sea through the Kattegat, strong vertical stratification, and high production /remineralization of OM due to eutrophication (Carstensen et al., 2014b; Conley et al., 2009). A permanent transition zone of about 2 to 10 m thickness separates the oxygenated surface and the oxygen-deficient waters, with a pelagic redoxcline located approximately between 127 and 129 m in GB, and between 79 and 85 m in LD (Glockzin et al., 2014). From the 1950s to 1970s, the hypoxic zones (<60 μM) in the Baltic Sea had expanded fourfold (Carstensen et al. 2014). Salt-water inflows from the North Sea are the primary mechanism renewing deep water in the central Baltic Sea (Günter et al., 2008). A Major Baltic Inflow (MBI) occurred in 2014/2015 (Mohrholz et al. 2015); this event ventilated bottom waters for five months between February and July 2015 (Holtermann et al., 2017). This MBI caused the intrusion of O<sub>2</sub> to deep hypoxic waters, substantial temperature variability (Holtermann et al., 2017), displacement of remnant stagnant water masses by new water that changed the chemistry of the water column (Myllykangas et al., 2017), and high turbidities that may be associated with redox reactions products (Schmale et al., 2016). At the time of sampling (June 2015), the MBI had reached GB but did not affect LD, located further northwest. The oxygenated water inflow reached GB at the beginning of March and created a secondary near-bottom redoxcline (Schmale et al., 2016); the bottom water anoxia started to re-established in July 2015 (Dellwig et al., 2018). In LD, water properties did not change due to the MBI, the sulfidic layer was maintained (hydrogen sulfide, H<sub>2</sub>S concentrations of 20.7- 21.2 μM), and salinity varied between 10.6 and 10.9 (Holtermann et al., 2017)."**

Line 109: this pelagic redoxcline is the original or the second redoxcline from the previous sentence?

*AR: This refers to the pelagic redoxclines in general. In hypoxic basins like the GB, there is regularly one pelagic redoxcline in the transition between the oxygenated surface and anoxic or even sulfidic*

*bottom waters. However, as a consequence of the MBI, a second pelagic redoxcline developed where there are the conditions for the same redox reactions to occur.*

**ACMS: L118-122, this sentence was modified to “Pelagic redoxclines are the suboxic transition between oxic and anoxic - even sulfidic- waters. A steep redox gradient characterizes this transition zone where electron acceptors and their reduced counterparts are vertically segregated, and biogeochemical transformations mediated by microbial processes are actively occurring (Bonaglia et al., 2016; Brettar and Rheinheimer, 1991; Neretin et al., 2003)”**

Line 114-115: “...under oxic conditions OR in the presence of nitrate they react with O<sub>2</sub> and ...” They will get oxidized, but in the latter case there is no O<sub>2</sub>?

*AR: We deleted this sentence since we modify the paragraph for clarity*

Line 127: TEP is or TEP particles are

*AR: TEP are defined as transparent exopolymeric particles. Therefore, TEP are is correct*

Line 133: by Stokes law...

*AR: We deleted “The” and the apostrophe of according to the editor suggestion*

**ACMS: L149-150, this sentence was modified to “by Stokes law”**

Line 161: special variability?

*AR: I don't understand the editor comment “special variability” in L161 or in any other place in the manuscript. Do you want me to add “special variability” in L161, I am not sure were...*

Line 173: filled up to 10 L? How much water did you have to add to get to 10 L. And why would you dilute your samples?

*AR: In general, after pooled ( ~0.6-0.8 L per tube) 12 tubes per depth together, we had to add approximately between 0.4 and 1.5 L. We standardize the final volume in order to be able to compare between depths following the procedure described in (Engel et al., 2017)*

**ACMS: L201-204, we modified the paragraph for clarity to “Then, we pooled together the remaining water, containing the sinking material (~0.6-0.8 L), of 12 tubes per depth into a large container, that we filled-up to 10 L with filtered seawater (between 0.4 and 1.5 L) to have the same volume per depth.”**

Line 174: swimmers were removed with a 500 µm mesh screen?

*AR: Yes, we use a 500 µm to screen the trapped material and remove the larger swimmers; this is one of the methods commonly used for swimmer removal (Buesseler et al., 2007; Conte et al., 2001). A reference was added to line 188*

**ACMS: L188, we added a reference “...the samples were screened with a 500 µm mesh to remove swimmers (Conte et al., 2001).”**

Line 185: Aliquots from the 10 L? So not only trapped material, but diluted trapped material?

*AR: We pooled together 12 tubes per depth, ~0.6-0.8 L per tube, this volume contains the trapped material already diluted in the saline solution that we added before deployment (50 g L<sup>-1</sup> of NaOH in 0.2 μm filtered seawater). The filtered seawater added to standardize the volume to 10 L per depth after recovery did not significantly increase the dilution of the trapped material. We measured the POM concentration in the saline solution, and we use that as a blank, the POM concentration was always negligible in the blank compared to the trapped material.*

**ACMS: L201-204, we modified the paragraph for clarity to “Then, we pooled together the remaining water, containing the sinking material (~0.6-0.8 L), of 12 tubes per depth into a large container, that we filled-up to 10 L with filtered seawater (between 0.4 and 1.5 L) to have the same volume per depth”**

Line 192: Did you define POP?

*AR: Yes, it is defined in L2014 (previously L184)*

Line 200-209: Am I correct in thinking that everything between 5 and 20 μm is both counted by flow cytometer and microscopy? I am assuming the flow cytometer is counting cells containing chlorophyll and/or phycoerythrin?

*AR: Yes, that is correct, although in practice the organisms quantified by microscopy ranged between 10 and 200 μm (L204); thus everything between 10 and 20 μm was counted by flow cytometer and microscopy.*

*As the editor points out, the flow cytometer is counting cells containing chlorophyll and/or phycoerythrin (L208)*

Line 214: Explain what coomassie normally stains. Later on explain why that might be interesting.

*AR: As we mention in our reply to the general comments, CSP are a protein containing exopolymeric particles that are abundant and ubiquitous in aquatic systems. CSP are stain with Coomassie Brilliant Blue, a dye commonly used to stain proteins (Bradford, 1976). We added a description of CSP in the introduction to define and explain their significance in this study. We also modified the methods section to better explain CSP.*

**ACMS: L155-161, we added a paragraph to the introduction explaining the significance of CSP in this study “Another type of less studied exopolymer particles are Coomassie stainable particles (CSP), they are protein-containing particles that stain with Coomassie brilliant blue (Long and Azam 1996). Little is known about the characteristics and dynamics of those particles in marine systems and their potential to form aggregates with MnOx had not been studied. Different to TEP, CSP have a limited role on the aggregation of diatoms (Prieto et al., 2002; Cisternas-Novoa et al., 2015), but seem to be important for the aggregation of cyanobacteria (Cisternas-Novoa et al., 2015).”**

**L234-235, we modified the sentence to “Polysaccharide (TEP) and protein (CSP) exopolymer particles, from sediment trap and water column samples were analyzed by microscopy according to Engel (2009).”**



**L231-233 “Alcian Blue solution, a dye that target acidic polysaccharides, for TEP or 1 mL of Coomassie brilliant blue solution, a dye commonly used to stain proteins (Bradford, 1976), for CSP.”**

Line 231-236: If this is a known method to measure particles containing MnOx, refer to these papers or methods. MnOx-like particles could basically be anything.

*AR: This point was explained in our reply to the general comments (1. Regarding MnOx-like particles)*

**ACMS: L252-266, we added a paragraph explaining how we identified and quantified MnOx-like particles: “MnOx-containing particles have been commonly identified based on their morphology, size and elemental composition, confirmed by scanning electron microscopy (SEM) and energy dispersive x-ray microanalysis (EDX) (Neretin et al., 2003; Glockzin et al., 2014; Dellwig et al., 2010, 2018). In this study, we did not measure the elemental composition of the particles. Thus, we identified them as “MnOx-like particles” based on similar morphology, size, and association with organic matter (OM) as MnOx-containing particles previously described in the Baltic Sea (eg., Neretin et al., 2003 and Glockzin et al., 2014). The abundance and size of MnOx-like particles were determined using particle recognition on filters and imaging processing similar to the method used by Neretin et al. (2003) but without the chemical composition analysis of the particles. For the image analysis, we used the same images as for TEP and CSP analysis and modified image analysis procedure described above as follows: thirty images per filter (200x) were analyzed semi-automatically using ImageJ software. After RGB split, the blue channel pictures were used to quantify MnOx-like particles in the water column and sediment traps. In this manner, the MnOx-like particles were clearly visible with a negligible disruption from TEP or CSP stained blue.”**

Line 243-244 “.... Undergoes degradation...”

*AR: We deleted “it” and “to”*

**ACMS: L274, this sentence was modified to “undergoes degradation”**

Line 272: The deepest point sampled in the LD (430 m)

*AR: We modified the sentence according to the editor’s recommendation*

**ACMS: L319-320, this sentence was modified to “from 74 m to the deepest point sampled in the LD (430 m)”**

Line 299: increased to 38.9

*AR: We the word “to”*

*(The line that the editor indicates (L299) did not coincide with the line numbered (L297) in the last version online form Nov 15, 2018)*

**ACMS: L343, this sentence was modified to “increased to 38.9”**

Line 301: the lowest concentration was not at 180 m?  
(L299)

*AR: No, H2S was not measurable at 300 and the lowest concentration was measured at 350 (0.04 μM), this coincide with a peak on NO2 (Fig2b).*

Line 304: GB  $\mu\text{g}$  per liter, LD  $\mu\text{g}$  per liter and  $\mu\text{M}$ ?

(L302)

AR: We deleted “and 0.1-0.3  $\mu\text{M}$ ”, it was a typo

**ACMS: L347, this sentence was modified to “in LD (1.4-1.2  $\mu\text{g L}^{-1}$ , Fig. 3e)”**

Line 304-312: There is overlap in your defined pico- and nanophytoplankton (< 20  $\mu\text{m}$ ) and large phytoplankton (> 5  $\mu\text{m}$ )?

(L309)

AR: We deleted “large” to avoid confusion due to the overlap; thus, we refer only to the different method that we use to quantify phytoplankton and not to their size.

**ACMS: L354, this sentence was modified to “Phytoplankton (>5  $\mu\text{m}$ ) abundance, determined by microscopy,)”**

**L355-356: “Filamentous cyanobacteria dominated the phytoplankton community at both stations with up to 90% corresponding to Aphanizomenon sp.”**

Line 314: Filament counts, so the actual biomass or even individual cell counts could be even way larger, right? This also means that the other spp are a percentage of the total **counts** or phytoplankton **counts**. Not of the total biomass or even cell counts. Completely dwarfed by the cyano’s therefore, right?

(L310)

AR: We agreed with the editor that the individual cell counts must be significantly larger. The other spp are a percentage of the phytoplankton counts (considering filament counts), which means a significant dominance of cyano.

Line 315: total counts, so you could wonder if they are indeed significant based on biomass or cell counts taking into account you counted filaments rather than cyano cells.

(L312)

AR: We deleted “total” to make clear that we are talking about phytoplankton counts in which we considering filament counts.

Line 317: total phytoplankton counts

Line 318: phytoplankton counts

AR: We are not sure if we could follow this correctly since the lines that the editor indicate did not coincide with the line numbered in the last version online form Nov 15, 2018. We deleted “total” to avoid confusion since we are always referring to the phytoplankton counts considering filament counts.

**ACMS:**

**L356 (previous L312) “represented 56% of the phytoplankton counts in the GB”**

**L358 (previous L313) “Dinoflagellates (dominated by Dinophysis sp.) were significant in both stations (19% of the phytoplankton counts)**

**L360 (previous L315) “(25% and 4% of the phytoplankton counts respectively)”**

Line 331: TEP particles were counted right? So shouldn’t this be counts as well?

AR: As described in the methods section (L244-247) “Additionally, TEP and CSP in water samples from the stations where we deployed sediment traps were analyzed spectrophotometrically (with higher

*vertical resolution than microscopy) according to Passow and Alldredge (1995) and Cisternas-Novoa et al. (2014), respectively”*

Line 340: so here is a little indication of what CSP might be... gel like, the question what it is still remains.

*AR: As explained above (please see replay for L214), we now described CSP, their protein-containing nature, and their significance for this study in the introduction; in addition, we add that Coomassie brilliant blue stains proteins in the methods section.*

Line 345: MnOx containing particles? But did you actually measure MnOx? Or just counted particles that looked and behave as MnOx?

*AR: As explained above (please see reply for L231-236), we now added a paragraph explaining how we identified and quantified MnOx-like particles (L252-266) to the methods section. Since we did not perform SED-EDX analysis (but counted and size particles that looked and behave as MnOx-containing particles in many ways, please see reply to general comments “1. Regarding MnOx-like particles”) we call the particles described in this study “MnOx-like particles” and compared them with the previously described MnOx-containing particles.*

Line 362-363: by 18%  
(L360-361)

*AR: We changed (18%) for by 18%*

**ACMS: L406, this sentence was modified to “POC flux slightly increased by 18% from the shallowest (40 m) to the deepest (180 m) sediment trap”**

Line 376: Fully oxygenated water depths  
(L374)

*AR: We added “water”*

**ACMS: L418-419, this sentence was modified to “MnOx-like particles were not observed in sediment trap samples collected in fully oxygenated waters depths (40 and 60 m)”**

Line 384-387: IS the TAA related to CSP?

*AR: CSP are protein-containing particles, but there is no information about their specific chemical composition, this limits our understanding of the relationship between CSP and amino acids. Considering our data there is not a significant relationship between TAA flux and CSP flux ( $r^2 = 0.2$ ,  $p = 1$ , not include in the ms).*

*On the other hand, since one of the sources of CSP are phytoplankton exudates, it could be expected that CSP were related to amino acids released by phytoplankton (Thornton et al., 2018). Diatoms commonly released serine, glycine, glutamic acid, aspartic acid, ornithine, and histidine (Mykkestad 2000); phytoplankton also releases fluorescent amino acids such as tryptophan, tyrosine, and phenylalanine.*

*In our data set, there is a significant relationship between CSP flux and the concentration of glutamic acid ( $r^2 = 0.73$ ,  $p < 0.01$ ), serine ( $r^2 = 0.70$ ,  $p < 0.01$ ), alanine ( $r^2 = 0.77$ ,  $p < 0.01$ ), aspartic acid ( $r^2 = 0.65$ ,  $p < 0.05$ ), tryptophan ( $r^2 = 0.64$ ,  $p < 0.05$ ), tyrosine ( $r^2 = 0.83$ ,  $p < 0.01$ ), and phenylalanine ( $r^2 = 0.77$ ,  $p < 0.01$ ). There was not a significant relationship with glycine, and we did not measure serine, histidine or ornithine.*

*However, since there is no studies about the actual amino acids content of CSP, those relationships may be interpreted with caution and further research focusing on the composition of CSP are needed to conclude in this respect.*

Line 398: SOM or DOM?

*AR: Aminoacids and sugars were measured in total organic matter (DOM +POM), we compared the ratios from the material collected in the water column, called suspended organic matter, vs the material collected in sediment traps, called sinking organic matter.*

**ACMS: L436-437, the opening sentence of this paragraph was modified for clarity “Comparing molar elemental ratios of sinking (from sediment trap material) and suspended (from water column) particles to the revisited Redfield ratio”**

Line 406: indicate the Redfield ratio for Si.

*AR: We add the Si to the modified Redfield ratio*

**ACMS: L437-438, the Redfield ratio was modified to “to the revisited Redfield ratio for living plankton (106C: 16N: 15Si: P; Redfield et al., 1963; Brzezinski, 1985)”**

Line 411: TCHO?

(L409)

*AR: We added the “T”*

**ACMS: L458-459, this sentence was modified to “Similarly, the carbon contained in TCHO made up a larger percentage in sinking than in suspended particles (Table 5)”**

Line 427: biomass? Or counts?

(L425)

*AR: We changes biomass for abundance (estimated by counting)*

**ACMS: L474-477, this sentence was modified to “Moreover, though there were slight differences between the stations concerning phytoplankton abundance and composition, and concentration and chemical composition of POM, in the surface water column, those were not significant.”**

Line 437: the overlap in size classes again?

(L435)

*AR: We changed “smaller” by “measured by flow cytometer” (L431) and we deleted “larger” (L435) to differentiate the phytoplankton quantified by different methods and not by size (consistently with the methods section)*

**ACMS: These sentence were modified to:**

**L480-482 (previously L455): “At both stations, the abundance of pico-phytoplankton (<2 μm) was an order of magnitude higher than nano-plankton (Table 2).”**

**L459 (previously L435): “Microscopic analysis of phytoplankton”**

Line 483: MnOx-like and in line 485 you are sure it is actually MnOx, what has changed?

(L481, L483)

*AR: In L481 we are referring to the particles measured in this study, “MnOx-like particles” while in L483 we refer to previous findings. We added the word “containing” and the citation for clarity.*

**ACMS: L544-545 (previously L483-482), these sentences were modified to “One consequence of those changes is the vertical extension of the layer in which MnOx-containing aggregates could form (Schmale et al., 2016);”**

Line 531-532: So in Glockzin et al they actually measure manganese?  
(L529-L530)

*AR: Yes, they measured particulate Mn in the water column and the Mn content in MnOx containing particles using SEM-EDX (Please see reply to general comments “1. Regarding MnOx like particles” for more details).*

**ACMS: we added a paragraph in the discussion explaining why our MnOx-like particles may correspond to the previously reported MnOx-containing particles:**

**L611-617: “The high flux of POC at GB coincided with the appearance of dark, star-shaped particles that we defined as MnOx-like particles, particularly evident at GB (Fig. 6a,b, and e), but also present in LD. Based on their morphology, size, and aggregation with OM, we propose that those particles correspond to MnOx-containing particles enriched in OM that have been previously described at GB (Neretin et al., 2003; Pohl et al., 2004; Glockzin et al., 2014; Dellwig et al., 2010, 2018) and LD (Glockzin et al., 2014; Dellwig et al., 2010).”**

Line 533: (H<sub>2</sub>S), pretty sure there is H<sub>2</sub>O.  
(L531)

*AR: We changed H<sub>2</sub>O to H<sub>2</sub>S*

**ACMS: L641-642, the sentence was modified to: “Below the oxycline, and due to the presence of H<sub>2</sub>S, the particulate Mn concentration decreased drastically.”**

Line 537-538: “... redox conditions favorable for the formation of MnOx resulting in the high MnOx flux measured ...”  
(L535-L536)

*AR: We changed this sentence according to the editor recommendation*

**ACMS: L646-648, these sentences were modified to: “...redox conditions favorable for the formation of MnOx, resulting in the high MnOx-like particles flux measured in the sediment trap located in the core of the OMZ (110 m) and at 180 m (oxygenated deep water)”**

Line 547: containing or should it be like?  
(L545)

*AR: We changed “MnOx-containing” to “MnOx-like” since we refer to the particles measured in this study*

**ACMS: L656-657, the sentence was modified to: “The presence of MnOx-like particles in aggregates (Fig 6a) may have implications for the vertical flux of POC, PN and POP in a stratified system with a pelagic redoxcline like the Baltic Sea.”**

Line 590: we consider  
(L588)

*AR: We changed “considered” to “consider”*

**ACMS: L698, the sentence was modified to: “If we consider a mixed aggregate ...”**

Line 592: mixed

(L590)

*AR: We changed "mix" to "mixed"*

**ACMS: L701, the sentence was modified to: "...the largest mixed aggregates composed of MnOx and TEP"**

Line 598: mixed

(L596)

*AR: We changed "mix" to "mixed"*

**ACMS: L706-707, the sentence was modified to: "There is no information about the amount of OM relatively to MnOx-containing particles in those mixed aggregates"**

Line 606: than rather than that?

(L604)

*AR: We changed "that" to "than"*

**ACMS: L632, the sentence was modified to: "OM export is different under anoxic than under oxic conditions in the Baltic Sea"**

Line 615: "... how similar the biogeochemical conditions were ..."

(L613)

*AR: We changed the sentence for clarity and accuracy*

**ACMS: L734-735, the sentence was modified to: "In the sections above we compared the biogeochemical conditions and the size of the POM pool in the euphotic zone of GB and LD."**

Line 625: Hence the N<sub>2</sub> fixing cyano's?

(L623)

*AR: We deleted this sentence, since it refer to the results of that particular study and the role of N<sub>2</sub> fixation in the C:N ratio is outside the scope of this manuscript.*

**ACMS: L741-743, the sentence was modified to: "Our measured values of POC:PN (~10) and POC:POP (between 89 and 506) in suspended OM coincide with the simulated ratio reported immediately after the culmination of the spring bloom by Kreuz et al. (2015)."**

Line 660: transporting solid material from the and ?

(L658)

*AR: We fixed this sentence*

**ACMS: L796-798, the sentence was modified to: "The 2014/2015 MBI supplied oxygen-rich waters to GB transporting solid material from shallower areas and modifying the O<sub>2</sub> vertical profile and the redox conditions in the otherwise permanent suboxic deep waters."**

Line 662: for the comparison of POM

(L660)

*AR: We changed the sentence according to the editor recommendation*

**ACMS: L798-800, the sentence was modified to: "This event did not affect LD allowing for the comparison of POM fluxes and composition under two different O<sub>2</sub> concentrations with similar surface water conditions."**

#### References:

- Bradford, M. M.: A rapid and sensitive method for the quantitation of microgram quantities of protein utilizing the principle of protein-dye binding, *Analytical Biochemistry*, 72, 248-254, 1976.
- Buesseler, K. O., Antia, A. N., Chen, M., Fowler, S. W., Gardner, W. D., Gustafsson, Ö., Harada, K., Michaels, A. F., Rutgers v. d. Loeff, M., Sarin, M., Steinberg, D. K., and Trull, T. W.: An assessment of the use of sediment traps for estimating upper ocean particle fluxes, *Journal of Marine Research*, 65, 345-416 . , 2007.
- Conte, M. H., Ralph, N., and Ross, E. H.: Seasonal and interannual variability in deep ocean particle fluxes at the Oceanic Flux Program (OFP)/Bermuda Atlantic Time Series (BATS) site in the western Sargasso Sea near Bermuda, *Deep Sea Research Part II: Topical Studies in Oceanography*, 48, 1471-1505, 2001.
- Dellwig, O., Leipe, T., März, C., Glockzin, M., Pollehne, F., Schnetger, B., Yakushev, E. V., Böttcher, M. E., and Brumsack, H.-J.: A new particulate Mn–Fe–P-shuttle at the redoxcline of anoxic basins, *Geochimica et Cosmochimica Acta*, 74, 7100-7115, 2010.
- Dellwig, O., Schnetger, B., Meyer, D., Pollehne, F., Häusler, K., and Arz, H. W.: Impact of the Major Baltic Inflow in 2014 on Manganese Cycling in the Gotland Deep (Baltic Sea), *Frontiers in Marine Science*, 5, 2018.
- Engel, A., Wagner, H., Le Moigne, F. A. C., and Wilson, S. T.: Particle export fluxes to the oxygen minimum zone of the eastern tropical North Atlantic, *Biogeosciences*, 14, 1825-1838, 2017.
- Glockzin, M., Pollehne, F., and Dellwig, O.: Stationary sinking velocity of authigenic manganese oxides at pelagic redoxclines, *Marine Chemistry*, 160, 67-74, 2014.
- Keil, R. G., Neibauer, J. A., Biladeau, C., van der Elst, K., and Devol, A. H.: A multiproxy approach to understanding the "enhanced" flux of organic matter through the oxygen-deficient waters of the Arabian Sea, *Biogeosciences*, 13, 2077-2092, 2016.
- Neretin, L. N., Pohl, C., Jost, G., Leipe, T., and Pollehne, F.: Manganese cycling in the Gotland Deep, Baltic Sea, *Marine Chemistry*, 82, 125-143, 2003.
- Thornton, D. C. O.: Coomassie Stainable Particles (CSP): Protein Containing Exopolymer Particles in the Ocean, *Frontiers in Marine Science*, 5, 2018.
- Van Mooy, B. A. S., Keil, R. G., and Devol, A. H.: Impact of suboxia on sinking particulate organic carbon: Enhanced carbon flux and preferential degradation of amino acids via denitrification, *Geochimica et Cosmochimica Acta*, 66, 457-465, 2002.





## Abstract

Particle sinking is a major form to transport photosynthetically fixed carbon below the euphotic zone via the biological carbon pump (BCP). Oxygen (O<sub>2</sub>) depletion may improve the efficiency of the BCP. However, the mechanisms by which O<sub>2</sub>-deficiency can enhance particulate organic matter (POM) vertical fluxes are not well understood. Here, we investigate the composition and vertical fluxes of POM in two deep basins of the Baltic Sea (GB: Gotland basin and LD: Landsort Deep). The two basins showed different oxygen regimes, resulting from the intrusion of oxygen-rich water from the North Sea that ventilated the water column below 140 m in GB, but not in LD. In June 2015, we deployed surface-tethered drifting sediment traps in oxic surface waters (GB: 40 and 60 m; LD: 40 and 55m), within the oxygen minimum zone (OMZ, GB: 110 m and LD: 110 and 180 m), and at recently oxygenated waters by the North Sea inflow in GB (180 m). The primary objective of this study was to test the hypothesis that the different O<sub>2</sub> conditions in the water column of GB and LD affected the composition and vertical flux of sinking particles, and caused differences in export efficiency between those two basins.

Composition and vertical flux of sinking particles were different in GB and LD. In GB, particulate organic carbon (POC) flux was 18% lower in the shallowest trap (40 m) than in the deepest sediment trap (at 180 m). Particulate nitrogen (PN) and Coomassie stainable particles (CSP) fluxes decreased with depth, while particulate organic phosphorus (POP), biogenic silicate (BSi), chlorophyll *a* (Chl *a*), and transparent exopolymeric particles (TEP) fluxes peaked within the core of the OMZ (110 m); this coincided with the presence of manganese oxide (MnOx)-like particles aggregated with organic matter. In LD, vertical fluxes of POC, PN, and CSP decreased by 28, 42 and 56% respectively, from the surface to deep waters. POP, BSi and TEP fluxes did not decrease continuously with depth, but they were higher at 110 m. Although we observe higher vertical flux of POP, BSi and TEP coinciding with abundant MnOx-like particles at 110 m in both basins, the peak in the vertical flux of POM and MnOx-like particles was much higher in GB than in LD. Sinking particles were remarkably enriched in BSi, indicating that diatoms were preferentially included in sinking aggregates and/or there was an inclusion of lithogenic Si

44 [\(scavenged into sinking particles\) in our analysis.](#) During this study, [the POC transfer efficiency](#)  
45 [\(POC flux at 180 m over 40 m\) was higher in GB \(115%\) than in LD \(69%\) suggesting that under](#)  
46 [anoxic conditions a smaller portion of the POC exported below the euphotic zone was transferred](#)  
47 [to 180 m than under re-oxygenated conditions present in GB. In addition, the vertical fluxes of](#)  
48 [MnOx-like particles were two orders of magnitude higher in GB than at LD.](#)

49 Our results suggest that [POM aggregate with](#) MnOx-like particles formed after the inflow of  
50 oxygen-rich water into GB, [the formation of those MnOx-OM rich particles](#) may [alter the](#)  
51 [composition and vertical flux of POM, potentially contributing to a](#) higher transfer efficiency of  
52 POC in GB. This idea is consistent with [observations of](#) fresher and less degraded [organic matter](#)  
53 [in deep waters of](#) GB than LD.

## 54 **1. Introduction**

55 [Particle sinking is](#) the primary [mechanism](#) for transporting photosynthetically fixed carbon [below](#)  
56 [the euphotic zone](#) via the [biological carbon pump \(BCP\)](#) (Boyd and Trull, 2007; Turner, 2015).  
57 [Previous studies suggested](#) that the transfer of particulate organic carbon (POC) from the euphotic  
58 zone to the ocean interior is enhanced in oxygen minimum zones (OMZs) (Cavan et al., 2017;  
59 Devol and Hartnett, 2001; Engel et al., 2017; Keil et al., 2016; Van Mooy et al., 2002). Possible  
60 mechanisms explaining the higher POC transfer include: i) the reduction of aggregate  
61 fragmentation due to the lower zooplankton abundance within the OMZ (Cavan et al., 2017; Keil  
62 et al., 2016); ii) [the potentially high contribution of](#) refractory [terrestrial organic matter \(OM\) to](#)  
63 [the POC flux](#) (Keil et al., 2016; Van Mooy et al., 2002); iii) a decrease in heterotrophic microbial  
64 activity due to oxygen ( $O_2$ ) limitation (Devol and Hartnett, 2001); iv) the preferential degradation  
65 of nitrogen-rich organic compounds (Kalvelage et al. 2013; Van Mooy et al. 2002, Engel et al.  
66 2017), and v) changes in ballast materials that may alter the sinking velocity and protect [OM](#) from  
67 degradation (Armstrong et al., 2002). [Currently, the study of POC vertical flux in OMZ's has](#)  
68 [been mostly focused on the tropical ocean](#) (Cavan et al., 2017; Devol and Hartnett, 2001; Engel et  
69 al., 2017; Keil et al., 2016; Van Mooy et al., 2002); [whereas](#), how low  $O_2$  concentration would

70 affect the composition and fate of sinking OM, and the efficiency of the [BPC](#) in oxygen-deficient  
71 [zones of temperate-boreal regimes such as the Baltic deep](#) basins [had been less studied](#).

72 The semi-enclosed, brackish Baltic Sea is a unique environment with strong natural gradients of  
73 salinity and temperature (Kullenberg and Jacobsen, 1981), primary productivity, nutrients  
74 (Andersen et al., 2017), and O<sub>2</sub> concentrations (Carstensen et al., 2014a). New production,  
75 defined as the fraction of the autotrophic production supported by allochthonous sources of  
76 nitrogen (Dugdale and Goering, 1967) is considered equivalent to the particulate OM export  
77 (Eppley and Peterson, 1979; Legendre and Gosselin, 1989) on appropriate timescales. In the  
78 Baltic Sea, new production varies seasonally (Thomas and Schneider, 1999); [with](#) periods of [high](#)  
79 new production [during spring and summer](#), -supported by the diatom-dominated spring bloom and  
80 by diazotrophic cyanobacteria, respectively (Wasmund and Uhlig, 2003). Based on sediment trap  
81 data, collected at 140 m depth in the Gotland Basin ([GB](#)), Struck et al. (2004) reported that the  
82 highest fluxes of POC [occurred](#) in fall, followed by summer and spring. Using  $\delta^{15}\text{N}$ , they showed  
83 that during the summer, N<sub>2</sub> fixation by diazotrophic species [is](#) the primary source (~41%) of the  
84 exported nitrogen and that the majority of the sedimentary particulate [organic matter](#)-([POM](#)) in  
85 the central Baltic Sea is of pelagic origin.

86 OM export from the euphotic zone to the seafloor has a dual significance in the deep basins of the  
87 Baltic Sea. On the one hand, it contributes to the long-term burial of POC, and consequently to  
88 the removal and long-term storage of CO<sub>2</sub> from surface waters (Emeis et al., 2000; Leipe et al.,  
89 2011), [and](#) on the other hand, it connects the pelagic and the benthic systems contributing to the  
90 [O<sub>2</sub>](#) consumption and hence deoxygenation at depth. Environmental and anthropogenic changes  
91 may alter the magnitude and composition of OM transferred from the surface to the seafloor in the  
92 Baltic Sea (Tamelander et al. 2017). The reduction of nutrient inputs as targeted by the Baltic  
93 Marine Environment Protection Commission (HELCOM) [may reduce](#) in OM downward flux and  
94 limit the oxygen depletion [at depth](#). However, [since hypoxia occurred naturally in the Baltic Sea](#)  
95 [due to physical processes, mitigating eutrophication will only decrease the spatial extent and](#)  
96 [intensity of the O<sub>2</sub> deficiency in the deep basins](#).

97 GB ([248 m](#)) and Landsort Deep (LD, [460 m](#)) are the deepest basins of the Baltic [Sea](#). [They](#) exhibit  
98 permanent bottom-water hypoxia (Conley et al. 2002), caused by a combination of limited water  
99 exchange with the North Sea through the Kattegat, strong vertical stratification, and high  
100 production /rem mineralization of OM due to eutrophication (Carstensen et al., 2014b; Conley et al.,  
101 2009). [A permanent transition zone of about 2 to 10 m thickness separates the oxygenated surface](#)  
102 [and the oxygen-deficient waters, with a pelagic redoxcline located approximately between 127](#)  
103 [and 129 m in GB, and between 79 and 85 m in LD \(Glockzin et al., 2014\)](#). From the 1950s to  
104 1970s, the hypoxic zones ( $<60 \mu\text{M}$ ) in the Baltic Sea had expanded fourfold (Carstensen et al.  
105 2014). Salt-water inflows from the North Sea [are](#) the primary mechanism renewing deep water in  
106 the central Baltic Sea ([Günter et al., 2008](#)). A Major Baltic Inflow (MBI) occurred in 2014/2015  
107 (Mohrholz et al. 2015); this event ventilated bottom waters for five months between February and  
108 July 2015 (Holtermann et al., 2017). [This](#) MBI caused the intrusion of  $\text{O}_2$  to deep hypoxic waters,  
109 substantial temperature variability (Holtermann et al., 2017), displacement of remnant stagnant  
110 water masses by new water that changed the chemistry of the water column (Myllykangas et al.,  
111 2017), and high turbidities that may be associated with redox reactions products (Schmale et al.,  
112 2016). At the time of sampling (June 2015), [the](#) MBI had reached [GB](#) but did not affect LD,  
113 located further northwest. [The oxygenated water inflow reached GB at the beginning of March](#)  
114 [and created a secondary near-bottom redoxcline \(Schmale et al., 2016\); the bottom water anoxia](#)  
115 [started to re-established in July 2015 \(Dellwig et al., 2018\)](#). In LD, water properties did not  
116 change due to the MBI, the sulfidic layer was maintained (hydrogen sulfide,  $\text{H}_2\text{S}$  concentrations  
117 of 20.7- 21.2  $\mu\text{M}$ ), and salinity varied between 10.6 and 10.9 (Holtermann et al., 2017).

118 [Pelagic redoxclines are the suboxic transition between oxic and anoxic - even sulfidic- waters. A](#)  
119 [steep redox gradient characterizes this transition zone were ~~here~~](#) electron acceptors and their  
120 reduced counterparts are vertically segregated, and biogeochemical transformations mediated by  
121 microbial processes are actively occurring (Bonaglia et al., 2016; Brettar and Rheinheimer, 1991;  
122 Neretin et al., 2003). For instance, iron (Fe) and manganese (Mn) undergo rapidly reversible  
123 transformations at the redox interface. [Mn is an essential electron donor and acceptor in redox](#)

124 processes -occurring at brackish, pelagic systems with anoxic conditions like the deep basins of  
125 the Baltic Sea. Redox conditions control the biogeochemical transformations between dissolved  
126 Mn<sup>2+</sup> and insoluble oxides and hydroxides of Mn<sup>4+</sup>. Under anoxic conditions dissolved -reduced  
127 Mn forms dominates, while in the presence of O<sub>2</sub> the formation of particulate manganese oxides  
128 (MnOx) is favored. The concentration of dissolved Mn may reach 0.3 μM in GB and a maximum  
129 value of about 3 μM in the LD (Dellwig et al., 2012). van Hulst et al. (2017) estimated an  
130 aggregation threshold for manganese oxides of 25 pM, and suggested that a minimal  
131 concentration of dissolved Mn is required for an efficient aggregation and removal of MnOx.  
132 Therefore, in GB and LD, the balance between dissolve Mn and the formation of MnOx is  
133 controlled by the O<sub>2</sub> availability- (e.g., Neretin et al., 2003). LD is characterized by a permanently  
134 stratified water column and sulfidic bottom waters; these conditions favored the accumulation of  
135 high concentrations of dissolved Mn (Dellwig et al., 2012).

136 In contrast, GB is periodically affected by lateral intrusions of O<sub>2</sub> and the oxygenation of deep  
137 water as a result of MBI that occur every one to four years (Matthäus and Franck, 1992), favoring  
138 the occurrence of MnOx containing particles. MnOx production may be microbially mediated  
139 (Richardson et al., 1988), or authigenic (Glockzin et al., 2014). In sulfidic waters, the reduction of  
140 MnOx with sulfide occurs within a scale of seconds to minutes (Neretin et al., 2003), and is  
141 inhibited by nitrate (Dollhopf et al., 2000). The oxygenation of the deep water of GB by the  
142 2014/2015 MBI combined with the release of Mn from the sediments into the water column (Lenz  
143 et al., 2015) generate appropriate conditions to enhance particulate MnOx formation and  
144 vertically expand the zone where they could be observed in the water column.

145 MnOx-containing particles have previously been observed at pelagic redoxclines in the Baltic Sea  
146 (Glockzin et al., 2014; Neretin et al., 2003). They are amorphous or star-shaped particles, and  
147 occur as single particles or form aggregates with OM (Neretin et al., 2003), specifically with  
148 transparent exopolymer particles (TEP) (Glockzin et al., 2014). The sinking velocity (0.76 m d<sup>-1</sup>)  
149 of those mixed aggregates containing MnOx and TEP was lower than what was predicted by  
150 Stokes law possibly due to their star-shaped morphology and the high OM content. TEP are

151 highly sticky, polysaccharide-rich particles that can enhance [particle aggregation rates](#) and the  
152 formation of marine snow (Engel, 2000; Logan et al., 1995). Thus, [the sinking of MnOx-OM](#)  
153 aggregates may contribute to the downward flux of POC. However, [high content of TEP relative](#)  
154 [to more dense particles could](#) reduce the density of marine aggregates and decrease their sinking  
155 velocity (Engel and Schartau, 1999). [Another type of less studied exopolymer particles are](#)  
156 [Coomassie stainable particles \(CSP\), they are protein-containing particles that stain with](#)  
157 [Coomassie brilliant blue \(Long and Azam 1996\). Little is known about the characteristics and](#)  
158 [dynamics of those particles in marine systems and their potential to form aggregates with MnOx](#)  
159 [had not been studied. Different](#)~~In contrast~~ [to TEP, CSP have a limited role on the aggregation of](#)  
160 [diatoms \(Prieto et al., 2002; Cisternas-Novoa et al., 2015\), but seem to be important for the](#)  
161 [aggregation of cyanobacteria \(Cisternas-Novoa et al., 2015\). Mixed MnOx-OM aggregates may](#)  
162 [affect the cycling of particle-reactive elements like phosphorus and trace metals via scavenging](#)  
163 [processes, and it has been proposed that they could act as carriers of bacteria in the redoxcline](#)  
164 [\(Dellwig et al., 2010\). To date, there are no measurements of the density of MnOx-OM](#)  
165 [aggregates, their potential ballast effect on sinking OM, or their biogeochemical role modifying](#)  
166 [the vertical flux of POM in the Baltic Sea.](#)

167 The objectives of this study are, first, to [determine](#) the amount and composition of particles  
168 sinking out of the euphotic zone [into the](#) deep basins of the Baltic Sea: GB and LD. Second, to  
169 study how the oxygenation of deep waters ( $\geq 140$  m) caused by the 2014/2015 MBI [may](#) affect the  
170 [vertical flux of sinking particles. We, therefore, compared GB affected by the MBI](#) with LD that  
171 was not affected and exhibited low O<sub>2</sub> concentration ( $\geq 74$  m) and [even](#) sulfidic conditions ( $\geq 180$   
172 m). We hypothesized [that the MBI that altered the water column chemistry and created different](#)  
173 O<sub>2</sub> conditions in GB compared with LD affected the [composition and vertical flux of sinking](#)  
174 [particles. Additionally, the higher](#) abundance and *in-situ* formation of MnOx-OM aggregates [may](#)  
175 [cause](#) differences in degradation and export of OM between those two [basins](#).

## 176 2. Methods

### 177 2.1. Sampling location and water column properties

178 Samples were collected during the BalticOM cruise in the Baltic Sea onboard the *RV Alkor* from  
179 June 3<sup>th</sup> to June 19<sup>th</sup>, 2015. We collected sinking particles using surface-tethered [drifting](#) sediment  
180 traps (Engel et al., 2017; Knauer et al., 1979) in GB and LD ([Table 1](#)). Additionally, water  
181 column samples (table 2) were collected using a Niskin-bottle rosette at the locations of the trap  
182 deployments. Temperature, salinity and O<sub>2</sub> concentration were determined at each station using a  
183 Sea-Bird (CTD) probe equipped with a [O<sub>2</sub> sensor](#) (Oxyguard, PreSens), calibrated with discrete  
184 samples measured using the Winkler method (Strickland and Parsons, 1968; Wilhelm, 1888).

## 185 *2.2. Sediment trap design and deployment*

186 We deployed two surface-tethered [drifting](#) sediment traps for two days in GB, and one day in LD  
187 (Fig.1). Each trap collected particles at four depths: [40 m \(two arrays were deployed to evaluate](#)  
188 [replicability of particle collection\)](#), [60 m](#) (55m in LD), [110 m](#) and 180 m (Table 1) to estimate  
189 POM fluxes to and within the OMZ. [40 m was considered as the base of the euphotic zone based](#)  
190 [on PAR measurements conducted during the cruise \(data not shown\). At each depth, 12 acrylic](#)  
191 [particle interceptor tubes \(PITs\) mounted in a PVC cross frame were deployed.](#) Each [PIT](#) was  
192 equipped with an acrylic baffle at the top to minimize the collection of swimmers (Engel et al.,  
193 2017; Knauer et al., 1979). The PITs were 7 cm in diameter and 53 cm in height with an aspect  
194 ratio of 7.5 and a collection area of 0.0038 m<sup>2</sup>. The cross frame and PITs were attached to a line  
195 that had a bottom weight and a set of surface and subsurface floats. The procedures for PIT  
196 preparation and sample recovery followed Engel et al. (2017). Shortly before deployment, each  
197 PIT was filled with 1.5 L of seawater previously filtered through a 0.2 µm pore size cartridge. A  
198 preservative solution of saline brine (50 g L<sup>-1</sup>) was added slowly to each PIT underneath the 1.5 L  
199 of filtered seawater, carefully keeping the density gradient. The PITs were kept covered until  
200 deployment and immediately after recovery to avoid contamination. After recovery, the density  
201 gradient was visually verified, and the supernatant seawater was siphoned off the PIT. Then, [we](#)  
202 [pooled together](#) the remaining water, containing the [sinking material \(~0.6-0.8 L\)](#), [of 12 tubes per](#)  
203 [depth into a large container, that we](#) filled-up to 10 L with filtered seawater [\(between 0.4 and 1.5](#)  
204 [L\) to have the same volume per depth.](#) After that, the samples were screened with a 500 µm mesh

205 | to remove swimmers\_(Conte et al., 2001). Subsequently, samples were split into aliquots that were  
206 | processed for the different biogeochemical analysis as described in Engel et al. (2017).

### 207 | 2.3. Biogeochemical analysis

208 | Nutrients were measured in seawater samples [collected in](#) the deployment stations. Ammonium  
209 | (detection limit [of](#) 0.05  $\mu\text{M}$ ) was measured directly on unfiltered seawater samples on board after  
210 | Solórzano (1969). Phosphate, nitrate, and nitrite (detection limit [of](#) 0.04  $\mu\text{M}$ ) were filtered  
211 | through a 0.2  $\mu\text{m}$  pore size and stored frozen until their analysis; samples were measured  
212 | photometrically with continuous flow analysis on an auto-analyzer (QuAAtro; Seal Analytical)  
213 | after Grasshoff et al. (1999).

214 | Particulate organic carbon (POC), nitrogen (PN), organic phosphorus (POP), and chlorophyll *a*  
215 | (Chl *a*) were determined as described in Engel et al. (2017). Aliquots, of 100 to 200 [mL](#) of the  
216 | trapped material and 500 [mL of the](#) seawater [samples](#), were filtered in duplicate for each  
217 | parameter at low vacuum (<200 mbar), onto pre-combusted GF/F filters (8h at 500°C). The filters  
218 | were stored frozen (-20°C) until analysis. Prior analysis, filters for POC-PN determination were  
219 | exposed to acid fumes (37% hydrochloric acid) to remove carbonates and subsequently dried for  
220 | 12h at 60 °C. POC and PN concentrations were determined using an elemental analyzer (Euro  
221 | EA, Hechatech) after Sharp (1974).

222 | POP was analyzed after Hansen and Koroleff (1999). POP was oxidized to orthophosphate by  
223 | heating the filters in 40 mL of deionized water (18.2M $\Omega$ ) with Oxisolv (MERCK 112936) for 30  
224 | min in a pressure cooker. Orthophosphate was determined spectrophotometrically at 882 nm in a  
225 | Shimadzu UV-VIS Spectrophotometer UV1201.

226 | Chl *a* was analyzed after extraction with 10 mL of 90% acetone, the fluorescence of the samples  
227 | was measured using a Turner [fluorometer](#) (440/685 nm, Turner, 10-AU) according to Strickland  
228 | et al. (1972). The fluorometer was calibrated with a standard solution of Chl *a* (Sigma-Aldrich C-  
229 | 5753).

230 | Biogenic silica (BSi) was determined [in aliquots of 50 to 100 mL, filtered in duplicate](#) onto 0.4  
231 |  $\mu\text{m}$  cellulose acetate filters. Samples were stored at -20°C until analysis. For the measurements,



232 filters were digested in NaOH at 85°C for 135 min; the pH was adjusted to 8 with HCl. Silicate  
233 was measured spectrophotometrically according to Hansen and Koroleff (2007).

234 [Polysaccharide \(TEP\) and protein \(CSP\) exopolymer particles](#), from [sediment](#) trap and water  
235 column [samples](#) were analyzed by microscopy according to [Engel \(2009\)](#). Duplicate aliquots of 5  
236 to 20 [mL](#) were filtered onto 0.4 µm Nuclepore membrane filters (Whatmann) and stained with 1  
237 [mL](#) of Alcian Blue solution, [a dye that target acidic polysaccharides](#), for TEP or 1 [mL](#) of  
238 Coomassie brilliant blue solution, [a dye commonly used to stain proteins](#) (Bradford, 1976), for  
239 CSP. Filters were transferred onto Cytoclear ® slides and frozen (-20°C) until microscopy  
240 analysis. For the analysis, thirty images for each filter were captured under 200x magnification  
241 using a light microscope (Zeiss Axio Scope A.1) connected to a color camera (AxioCam MRc).  
242 Particle abundance and area were measured semi-automatically using an image analysis system  
243 including the WCIF ImageJ software. The RGB was split [into](#) three channels: red, blue and green,  
244 and the red was used to quantify the amount of TEP and CSP. Additionally, TEP and CSP in  
245 water samples from the stations where we deployed sediment traps were analyzed  
246 spectrophotometrically (with higher vertical resolution than microscopy) according to Passow and  
247 Alldredge (1995) and Cisternas-Novoa et al. (2014), respectively. Concentrations of TEP are  
248 reported relative to a xanthan gum standard and expressed in micrograms of xanthan gum  
249 equivalents per liter ( $\mu\text{g XG eq. L}^{-1}$ ), and concentrations of CSP are reported relative to a bovine  
250 serum albumin standard and expressed in micrograms of bovine serum albumin equivalents per  
251 liter ( $\mu\text{g BSA eq. L}^{-1}$ ).

252 [MnOx-containing particles have been commonly identified based on their morphology, size and](#)  
253 [elemental composition, confirmed by scanning electron microscopy \(SEM\) and energy dispersive](#)  
254 [x-ray microanalysis \(EDX\) \(Neretin et al., 2003; Glockzin et al., 2014; Dellwig et al., 2010,](#)  
255 [2018\). In this study, we did not measure the elemental composition of the particles. Thus, we](#)  
256 [identified them as "MnOx-like particles" based on similar morphology, size, and association with](#)  
257 [organic matter \(OM\) as MnOx-containing particles previously described in the Baltic Sea \(eg.,](#)  
258 [Neretin et al., 2003 and Glockzin et al., 2014\).](#) The abundance [and size](#) of MnOx-like particles

259 | were determined [using particle recognition on filters and imaging processing similar to the](#)  
260 | [method used by Neretin et al. \(2003\) but without the chemical composition analysis of the](#)  
261 | [particles. For the image](#) analysis, [we used](#) the same images [as](#) for TEP and CSP analysis and  
262 | modified [image analysis procedure](#) described above [as follows:](#) thirty images per filter (200x)  
263 | were analyzed semi-automatically using ImageJ [software](#). [After RGB split,](#) the blue channel  
264 | [pictures](#) [were](#) used to quantify MnOx-like particles in the water column and sediment traps. In this  
265 | manner, the MnOx-like particles were clearly visible with a negligible disruption from TEP or  
266 | CSP stained blue.

267 | Total [hydrolyzable](#) amino acids (TAA) were analyzed in unfiltered seawater and trapped material.  
268 | Samples were stored at -20°C until analysis. Duplicate samples were hydrolyzed at 100 °C in 6N  
269 | HCl (Suprapur® Hydrochloric acid 30%) and 11 mM ascorbic acid for 20h. Amino acids were  
270 | separated and measured by high-performance liquid chromatography (HPLC), after derivatization  
271 | with ortho-phthaldialdehyde using a fluorescence detector (Excitation/Emission 330/445 nm)  
272 | (Dittmar et al., 2009; Lindroth and Mopper, 1979). [TAA concentrations were reported as μM of](#)  
273 | [monomer](#). The quantitative degradation index (DI) of Dauwe et al. (1999), based on changes in  
274 | amino acids composition of POM as [it](#) undergoes degradation processes, was calculated using the  
275 | factor coefficient of Dauwe et al. (1999) and the average and standard deviation of the TAA of  
276 | this data set.

277 | Total combined carbohydrates (TCHO) [> 1 kDa](#) were determined by [HPAEC-PAD](#) according to  
278 | Engel and Händel (2011). TCHO were analyzed in the unfiltered seawater and sediment trap  
279 | material. Samples were stored at -20°C until analysis. Prior to analysis, the samples were desalted  
280 | by membrane dialysis using dialysis tubes with 1 kDa molecular weight cut-off (Spectra Por).  
281 | [Desalination](#) was conducted for 4.5h at 1°C. Then, a 2 mL subsample was sealed with 1.6 mL [of](#)  
282 | 1M HCl in pre-combusted glass ampoules and hydrolyzed for 20h at 100°C. After hydrolysis, the  
283 | subsamples were neutralized by acid evaporation under N<sub>2</sub> atmosphere at 50°C, resuspended with  
284 | ultrapure Milli-Q water and analyzed [on a Dionex 3000 ion chromatography system](#). [TCHO](#)  
285 | [concentrations were reported as μM of monomer](#).

#### 286 | [2.4 Phytoplankton abundance](#)

287 Phytoplankton composition and abundance at the stations where we deployed sediment traps were  
288 evaluated using light microscopy and flow cytometry. Counts of phytoplankton cells > 5 µm,  
289 were made from 50 mL of fixed samples (Lugol's solution, 1% final concentration). Samples were  
290 concentrated using gravitational settling and counted under a Zeiss Axiovert inverted microscope  
291 (200x magnification) following the guidelines for determination of phytoplankton species  
292 composition, abundance (HELCOM, 2012). The counts were made on either half (cyanobacteria,  
293 diatoms, and *Dinophysis sp.*) or two strips (chryptophyta, unidentified dinoflagellates, and  
294 chlorophyta) of the chamber. Individual filaments of cyanobacteria were counted in 50 µm length  
295 units. The size of the counted phytoplankton species ranged from 10 to 200 µm.

296 Phytoplankton, <20 µm, cell abundance was quantified using a flow cytometer (FACSCalibur,  
297 Becton, Dickson, Oxford, UK). 2 mL samples were fixed with formaldehyde (1% final  
298 concentration) and stored frozen (-80 °C) until analysis (two weeks later). Red and orange  
299 autofluorescence were used to identify chlorophyll and phycoerythrin cells. Cell counts were  
300 determined with CellQuest software (Becton Dickenson); pico- and nanoplankton populations of  
301 naturally containing chlorophyll and/or phycoerythrin (*i.e.*, *Synechococcus*) were identified and  
302 enumerated.

### 303 2.5 Statistics

304 Significant differences between two parameters were tested using the Mann-Whitney U-test. The  
305 results of statistical analyses were assumed to be significant at  $p$ -values < 0.05. Statistical  
306 analyses were performed using Matlab software (MatlabR2014a).

## 307 3. Results

### 308 3.1. Biogeochemistry of the water column

309 At both stations, GB and LD, the water column was stratified during the study. In GB, the  
310 seasonal thermocline was located between 22 and 37 m, with temperature decreasing rapidly from  
311 9.8°C in the surface mix layer to 4.7°C below 37 m (Fig. 2a). Deeper in the water column, a  
312 pycnocline (halocline) coincided with the oxycline and was located between 65 m (S=7.6) and 80  
313 m (S=10.2); below 80 m the salinity gradually increased up to 13.5 (220 m). A hypoxic layer

314 (<40  $\mu\text{M O}_2$ ) was located between 74 and 140 m; the core of the OMZ (<10  $\mu\text{M O}_2$ ) was located  
315 between 96 and 125 m. The  $\text{O}_2$  concentration [increased](#) from 35  $\mu\text{M O}_2$  at 140 m to 79  $\mu\text{M O}_2$  at  
316 220 m (Fig. 2a). In LD, the seasonal thermocline was located between 10 and 39 m, where the  
317 temperature decreased gradually from 12°C to 4.0°C (Fig. 2b). The pycnocline was between 55  
318 (S=7.2) and 75 m (S=9) below that the salinity [was](#) constant (S=10.7) until the bottom of the  
319 station (430 m). The  $\text{O}_2$  concentration was below the detection limit (<3  $\mu\text{M O}_2$ ) from 74 m to the  
320 [deepest point sampled in LD \(430 m\)](#).

321 The vertical profile of nutrients was different at both stations (Fig. 2). In GB, nitrate concentration  
322 increased from below the detection limit in the upper ten meters to 0.17  $\mu\text{M}$  at 40 m (Fig. 2a).  
323 Concentrations were variable within the OMZ with 6  $\mu\text{M}$  in the upper (80 m) and lower oxycline  
324 (140 m), and 0.12  $\mu\text{M}$  in the core of [the](#) OMZ (110 m). Nitrate concentration [was](#) 4.8  $\mu\text{M}$  in the  
325 deepest sample (220 m). Nitrite was below the detection limit in most of the water column except  
326 for 60 m (0.09  $\mu\text{M}$ ) and 110 m (0.11  $\mu\text{M}$ ). Ammonium increased from 0.14  $\mu\text{M}$  in [the](#) upper ten  
327 meters to 1.15  $\mu\text{M}$  at 40 m; concentrations were variable [within](#) the OMZ with less than 0.15  $\mu\text{M}$   
328 in the upper (80 m) and lower oxycline (140 m), and maximum concentration of 3.28  $\mu\text{M}$  in the  
329 core of the OMZ (110m). Vertical profiles of phosphate and silicate at GB were similar; the  
330 concentrations steadily increased from the upper ten meters of the water column (0.29  $\mu\text{M}$  and  
331 10.36  $\mu\text{M}$ , respectively) to the OMZ (2.67  $\mu\text{M}$  and 39.07  $\mu\text{M}$ , respectively), and gradually  
332 decreased below the OMZ (Fig. 2a).  $\text{H}_2\text{S}$  was not detectable in GB.

333 In LD, nitrate and nitrite concentrations were below the detection limit between the surface and  
334 250 m (<0.04  $\mu\text{M}$ ) (Fig. 2b). Nitrite showed a maximum of 0.22  $\mu\text{M}$  at 350 m, and nitrate a  
335 maximum of 6.0  $\mu\text{M}$  at 400 m. Ammonium concentrations varied between 0.06 and 0.59  $\mu\text{M}$  in  
336 the upper 70 m and increased to 5.97 and 8.03  $\mu\text{M}$  in the OMZ ( $\geq 74$  m). The lowest [ammonium](#)  
337 concentration (0.07  $\mu\text{M}$ ) was measured in the surface and [the highest](#) (8.03  $\mu\text{M}$ ) at 110 m.

338 Phosphate and silicate concentrations were relatively low within the mixed layer; gradually  
339 increased below the pycnocline, and decreased [again](#) between 110 and 180 m. Phosphate  
340 concentrations varied between 1.5 and 2.5  $\mu\text{M}$  in the upper 110 m of the water column, decreased

341 to 0.22  $\mu\text{M}$  at 180 m and increased to 2.7  $\mu\text{M}$  at 430 m (deepest sample). Silicate ranged between  
342 25 and 38  $\mu\text{M}$  in the upper 110 m of the water column, decreased to 7.4  $\mu\text{M}$  at 180 m, and  
343 increased [to](#) 38.9  $\mu\text{M}$  at 430 m.  $\text{H}_2\text{S}$  was detectable below 180 m, with the highest concentration  
344 (3.97  $\mu\text{M}$ ) at 250 m and the lowest (0.04  $\mu\text{M}$ ) between 300 and 350 m (Fig. 2b).

### 345 *3.2. Particulate organic matter concentration in the water column*

346 Chl *a* concentration in the upper 10 m was slightly higher in GB (1.5-1.7  $\mu\text{g L}^{-1}$ , Fig. 3b) than in  
347 LD (1.4-1.2  $\mu\text{g L}^{-1}$ , Fig. 3e). [At](#) both stations, more than 90% of the total smaller phytoplankton  
348 (<20  $\mu\text{m}$ , pico- and nanophytoplankton) abundance, determined by flow cytometry, were  
349 measured in the upper 60 m, although phytoplankton was detectable in the entire water column.  
350 Pico- and nanophytoplankton abundances were 10% higher in GB than in LD (Table 2).

351 Picocyanobacteria determined by phycoerythrin fluorescence accounted [ed](#) for 92% and 96% of the  
352 total picophytoplankton [abundance](#) in GB and LD, respectively. Picocyanobacteria [abundance](#)  
353 was 30% higher in GB than in LD.

354 [Phytoplankton](#) (>5  $\mu\text{m}$ ) abundance, determined by microscopy, was 63% higher in LD than in GB  
355 (Table 3). Filamentous cyanobacteria dominated the phytoplankton community at both stations  
356 with up to 90% corresponding to *Aphanizomenon* sp. Cyanobacteria represented 56% of the  
357 phytoplankton counts in GB and up to 74% in LD. [Dinoflagellates \(including mixotrophs\)](#),  
358 dominated by *Dinophysis* sp, were significant in both stations (19% of the [phytoplankton counts](#)),  
359 whereas chlorophytes (dominated by filaments of *Planctonema* sp. containing cylindrical cells)  
360 were more abundant in GB than in LD (25% and 4% of the phytoplankton [counts](#) respectively).  
361 Diatoms represented less than 1% of the phytoplankton in both stations, and they were slightly  
362 more abundant at 40 m in LD (Table 3). BSi was higher in the upper 10 m (0.4-0.5  $\mu\text{M}$ ) and  
363 decreased with depth in GB (Fig. 3b), whereas in LD, BSi showed a peak at 40 m and then  
364 decreased with depth (Fig. [3e](#)).

365 Vertical profiles of POC, PN, and POP concentration were similar in the water column of the two  
366 stations (Fig. 3a, d). In GB, the concentrations were higher in the upper 10 m of the water column  
367 (POC:  $40.38 \pm 0.80$ , PN:  $3.89 \pm 0.01$ , and POP:  $0.26 \pm 0.04 \mu\text{M}$ ) and decreased gradually with

368 depth until 110 m where relatively high concentrations (POC  $18 \pm 0.63$ , PN:  $2 \pm 0.08$ , and POP:  
369  $0.2 \mu\text{M}$ ) were observed. The lowest concentrations were found at 180 m (POC:  $11.97 \pm 1.03$ , PN:  
370  $1.05 \pm 0.02$ , and POP  $< 0.03 \mu\text{M}$ ) (Fig. 3a). In LD, POM decreased with depth from the surface  
371 (POC:  $35 \pm 0.99$ , PN:  $4 \pm 0.09$ , and POP:  $0.2 \mu\text{M}$ ) to 40 m, remained relatively constant between  
372 40 and 80 m and decreased again between 110 and 250 m (Fig. 3d).

373 We observed high concentrations of TEP and CSP in the upper 10 m in both stations. The highest  
374 TEP concentration was [determined](#) at 1 and 10 m at both stations, and it was slightly higher (19%)  
375 in GB than in LD (Fig. 3c, f). TEP and CSP vertical profiles were different from each other in GB  
376 (Fig. 3c) and covaried in LD (Fig. 3f). Like observed for POC, PN, and POP, TEP concentrations  
377 showed a peak at 110 m ( $50.29 \pm 6.17 \mu\text{g XG eq. L}^{-1}$ ) in GB. The highest concentration of CSP at  
378 this station was observed in the shallowest (1 m) sample, CSP concentration decreased quickly  
379 below 10 m, and then it increased at 140 and [220 m \(the deepest sample, approximately 28 m](#)  
380 [above the seafloor\)](#) (Fig. 3c). In LD, the highest concentrations of TEP and CSP were measured [at](#)  
381 [the](#) surface (1 and 10 m) and at 110 m (Fig. 3f). TEP and CSP decreased with depth in the first 80  
382 m (from  $53.26 \pm 7.10$  to  $18.39 \pm 4.57 \mu\text{g XG eq. L}^{-1}$  and from  $53.26 \pm 7.10$  to  $31.57 \pm 18.78 \mu\text{g BSA}$   
383  $\text{eq. L}^{-1}$ ). Both types of gel-like particles showed an increase in concentration at 110 m ( $49.25 \pm$   
384  $4.08 \mu\text{g XG eq. L}^{-1}$  and  $66.89 \pm 22.33 \mu\text{g BSA eq. L}^{-1}$  respectively). Below 110 m, TEP  
385 concentrations stayed relatively constant, while CSP concentrations decreased at 180 m and kept  
386 relatively constant below that depth.

### 387 *3.3. MnOx-like particles vertical distribution in the water column*

388 Dark, star-shaped, MnOx-like particles (Glockzin et al., 2014; Neretin et al., 2003) were only  
389 observed below the fully oxygenated mixed layer in GB and, in less abundance, in LD (Fig. 4). In  
390 GB, [MnOx-like particles were observed from 80 m to 220 m; they appear as single particles](#) and  
391 [forming large aggregates containing several MnOx-like particles associated with OM](#). Relatively  
392 high concentration of MnOx-like particles ( $2 \times 10^6$  particles  $\text{L}^{-1}$ ) were [observed](#) in the upper (80 m,  
393 [25  \$\mu\text{M O}\_2\$](#) ) and lower (140 m, [36  \$\mu\text{M O}\_2\$](#) ) oxycline, and at 220 m, [79  \$\mu\text{M O}\_2\$](#)  ( $4 \times 10^6$  particles  $\text{L}^{-1}$ )  
394 (Fig. 4a). The lowest abundance of MnOx-like particles ( $7 \times 10^5$  particles  $\text{L}^{-1}$ ) was observed at

395 | 110 m, [6  \$\mu\text{M O}\_2\$](#) , [i.e.](#) in the core of the OMZ. The equivalent spherical diameter (ESD) [of MnOx-](#)  
396 | [like particles](#) varied between 0.6 and 30.5  $\mu\text{m}$ , [with a](#) median [size of](#) 3.0  $\mu\text{m}$ . The largest  
397 | aggregates [\(up to 30.5  \$\mu\text{m}\$ \)](#) were observed in the upper oxycline (80 m). In LD, MnOx-like  
398 | particles were less abundant, smaller, and had a narrow distribution in the water column than in  
399 | GB. MnOx-like particles were not detected in the fully oxic (0-40 m) or fully anoxic (180 to 430  
400 | m) water column. At 60 m ([135  \$\mu\text{M O}\_2\$](#) ), right above the oxycline, MnOx-like particles began to  
401 | appear, however, in relatively low abundance. The maximum abundance [of MnOx-like particles](#),  
402 |  $9 \times 10^5 \text{ L}^{-1}$ , was observed in the oxycline at 70 m ([27  \$\mu\text{M O}\_2\$](#) , Fig. 4b). The ESD ranged between  
403 | 0.6 and 13.4  $\mu\text{m}$ , the largest aggregates were observed at 70 m.

#### 404 | 3.4. [Vertical flux of Sinking Particles](#)

405 | [Vertical](#) fluxes of POC and PN varied little with depth in GB (Fig. 5a). POC flux slightly  
406 | increased [by](#) 18% from the shallowest (40 m) to the deepest (180 m) sediment trap. Fluxes of PN  
407 | [\(Fig. 5a\)](#) and CSP [\(Fig. 6b\)](#) were higher at 40 and 60 m and decreased (19 and 70 %) from 60 to  
408 | 180 m respectively. On the other hand, fluxes of POP, BSi, Chl *a* (Fig. 5b) and TEP (Fig. 6a)  
409 | peaked in the sediment trap located in the core of the OMZ (110 m). The increment of fluxes at  
410 | 110 m coincided with the [high abundance](#) of MnOx-like particles associated with TEP (Fig. 6a).  
411 | In addition, TEP size distribution, determined by image analysis, indicated an increase in large  
412 | TEP at 110 m (data not shown). In contrast, in LD, POC, PN (Fig. [5c](#)) and CSP (Fig. 6d) fluxes,  
413 | steadily decreased with depth by 28, 42 and 56% from 40 to 180 m. Similar to the fluxes  
414 | measured in GB, the POP, BSi (Fig. [5d](#)) and TEP (Fig. 6c) showed a smaller peak in the sediment  
415 | trap located at 110 m.

416 | MnOx-like particles were drastically less abundant in sediment trap samples from LD than in GB,  
417 | and when present, they appeared [ed](#) as single particles, not aggregated with TEP or CSP (Fig. 6c, d).  
418 | At both stations, and similar to the water column samples, MnOx-like particles were not observed  
419 | in sediment trap samples collected in fully oxygenated [waters](#) (40 and 60 m). The flux of MnOx-  
420 | like particles at 110 and 180 m was two orders of magnitude larger in GB than in LD (Table 4). In  
421 | GB, MnOx-like particles occurred as single particles [as well as](#) aggregates with each other and

422 OM such as TEP and CSP (Figure 6a,b, and e), phytoplankton cells, or detrital material. The ESD  
423 of MnOx-like particles and aggregates collected in the traps ranged from 0.6 to 167  $\mu\text{m}$  (median  
424 2.8  $\mu\text{m}$ ) at 110 m and from 0.6 to 153  $\mu\text{m}$  (median 3.3  $\mu\text{m}$ ) at 180 m. In LD, only a few, single  
425 MnOx-like particles were observed at 110 m (Fig. 6 c, d), their size ranged from 0.6 to 16.5  $\mu\text{m}$   
426 (median 1.8) (Table 4).

427 TAA flux ranged from  $371 \pm 12$  to  $501 \pm 33 \mu\text{mol m}^{-2}\text{d}^{-1}$  in GB and from  $502 \pm 84$  to  $785 \pm 54 \mu\text{mol}$   
428  $\text{m}^{-2}\text{d}^{-1}$  in LD (Fig. 7a). In GB, the flux steadily decreased from surface to depth, whereas in LD  
429 the TAA flux at 40 m was lower than at 60 m and decreased with depth from 60 to 180 m (Fig.  
430 7b). The vertical profile of TCHO flux was similar in both stations, although the magnitude of the  
431 flux was higher at LD. The TCHO flux varied between  $303 \pm 8$  and  $428 \pm 14 \mu\text{mol m}^{-2}\text{d}^{-1}$  in GB  
432 (Fig. 7a) and between  $503 \pm 19$  and  $584 \pm 8 \mu\text{mol m}^{-2}\text{d}^{-1}$  in LD (Fig. 7b). At both stations, TCHO  
433 fluxes increased from 40 to 110 m, where the highest flux was measured, and then it decreased at  
434 180 m.

### 435 3.5. Chemical composition of sinking and suspended particles

436 Comparing molar elemental ratios of sinking (from sediment trap material) and suspended (from  
437 water column) particles to the revisited Redfield ratio for living plankton (106C: 16N: 15Si: P;  
438 Redfield et al., 1963; Brzezinski, 1985), our results showed that the POC:PN ratio of sinking  
439 particles was slightly above this ratio at both stations. The POC:PN ratios of sinking particles in  
440 GB and LD were not significantly different. In GB however, ratios increased with depth from 9.8  
441 to 12.6, while in LD it varied between 11.1 and 15.4 without a clear trend with deep. The  
442 POC:POP ratios of sinking particles was lower ( $p < 0.05$ ; Mann–Whitney U-test) in GB (90.1-244)  
443 than in LD (230-772) with the highest value observed at 40 m and the lowest at 110 m. At both  
444 stations the POC:BSi ratios varied between 1.7 and 4.2 and PN:BSi ratios varied between 0.2 and  
445 0.4; the lowest values were observed at 110 m (Table 5).

446 Contrastingly, in suspended particles, POC:PN ratios were higher in GB than in LD ( $p < 0.001$ ). In  
447 GB, it varied between 8.4 and 12 without a clear trend with depth; while in LD, it decreased with  
448 depth from 8.7 (at 1m) to 6.2 (at 400\_m), and a slightly higher value of 7.8 was observed at 430 m.



449 The POC:PN and POC:POP were significantly higher ( $p < 0.01$ ) in sinking than in suspended  
450 particles (Table 5). The POC:BSi and the PN:BSi ratios were much lower in sinking than in  
451 suspended particles at both stations (GB:  $p < 0.05$ ; LD:  $p < 0.01$ ). In sinking particles, the POC:BSi  
452 ratio was below Redfield ratio of 7, whereas it was one to two orders of magnitude higher in  
453 suspended particles (Table 5). The PN:POP ratio was significantly lower in sinking (0.15-0.43)  
454 than in suspended particles (9.7-44.5) at both stations ( $p < 0.001$ ). In sinking particles, it was  
455 always below the Redfield ratio of 16, while in suspended particles, it was in the range of  
456 Redfield ratio in the upper 80 m in GB and always above in LD.

457 At both stations, the contribution of AA to POC was more significant in sinking than in  
458 suspended particles. Similarly, the carbon contained in TCHO made up a larger percentage in  
459 sinking than in suspended particles (Table 5). The amino acid-based degradation index (DI,  
460 Dauwe et al., 1999) varied from 0.1 to 1.14 in sinking OM and was higher than in suspended OM  
461 ( $-1.25$  to  $-0.42$ ) in both stations. In sinking OM, the DI decreased with depth in GB, whereas in  
462 LD, there was not a clear trend with depth (Table 5). The DI was higher in GB than in LD in  
463 sinking as well as in suspended OM.

#### 464 **4. Discussion**

465 In this study, we 1) characterized the biogeochemistry of the water column and the sinking  
466 particles in GB and LD, during early summer 2015, and 2) determined the vertical flux of sinking  
467 particles in those two deep basins of the Baltic Sea. Our results suggested that the intrusion of  
468 oxygenated water to GB, as consequence of the 2014/2015 MBI, caused changes in the water  
469 chemistry that affected the chemical composition and degradation stage of the sinking and  
470 suspended particles. Consequently, the composition and magnitude of the sinking particle flux  
471 were different in GB and LD.

#### 472 *4.1 Physical and biogeochemical conditions in GB and LD*

473 In general, physical and biogeochemical conditions (temperature, salinity, O<sub>2</sub>, and inorganic  
474 nutrient concentrations) were similar in the euphotic zone of both stations. Moreover, though  
475 there were slight differences between the stations concerning phytoplankton abundance and

476 [composition](#), and concentration and chemical composition of POM, in the surface water column,  
477 those were not significant. The concentration of Chl *a* (Fig. 3) and the abundance of [pico-](#) and  
478 [nano-phytoplankton](#) (Table 2) were slightly higher (20 and 10 % respectively) in GB than in LD.  
479 This agrees with estimates of integrated total primary production ([PP](#)), which were 10% [higher](#) in  
480 GB (380 mg C m<sup>-2</sup> d<sup>-1</sup>) than in LD (334 mg C m<sup>-2</sup> d<sup>-1</sup>; Piontek et al., unpublished). At both  
481 stations, [the abundance of](#) [pico-phytoplankton \(<2 μm\)](#) [was an order of magnitude higher than](#)  
482 [nano-plankton](#) (Table 2). These findings coincided with what was described previously for early  
483 summer in the Baltic Sea that indicate that during this period the productivity is sustained mostly  
484 by [pico- and nano-phytoplankton](#) communities (Leppänen et al., 1995) which co-existed with  
485 cyanobacteria and other phytoplankton species (Kreus et al. 2015). Microscopic analysis, on the  
486 other hand, [indicated that phytoplankton \(>5 μm\) abundance was 47% higher in LD than in GB.](#)  
487 [At both stations,](#) filamentous cyanobacteria ([> 90% \*Aphanizomenon\* sp.](#)) [were numerically](#) the  
488 [predominant type \(55 and 74% of the phytoplankton counts in GB and LD respectively\),](#)  
489 [dinoflagellates \(including mixotrophs\) correspond to 20%, and diatoms correspond to >1% of the](#)  
490 [phytoplankton abundance in the upper 40 m \(Table 3\). Diatoms were slightly higher in LD than in](#)  
491 [GB, and this coincide with a small peak in BSi concentration \(1.5 μM, Fig. 3e\) at 40 m in LD.](#)  
492 [Although at both stations the diatoms proportion from the total phytoplankton abundance was](#)  
493 [negligible, they could make a difference in the composition of sinking particles leaving the](#)  
494 [euphotic zone in LD due to selective aggregation of diatoms \(Passow et al., 1991\); however, in](#)  
495 [both stations sinking particles showed a similar enrichment in BSi. The low abundance of diatoms](#)  
496 [relative to cyanobacteria in the euphotic zone indicated that at both stations, the spring bloom was](#)  
497 [terminated and cyanobacteria were starting to build up the summer bloom that generally occurs in](#)  
498 [June-July \(Kreus et al., 2015\); \*Aphanizomenon\* sp. and \*Nodularia spumigena\*, are known to form](#)  
499 summer blooms, where they accumulate at the sea surface of the thermally stratified water  
500 column (Bianchi et al., 2000; Nausch et al., 2009; Wasmund, 1997).

501 [The concentration of particulate elements](#) (POC, PN, POP, BSi) [was](#) slightly higher in the surface  
502 waters of GB [compared to](#) LD; while [polysaccharide \(TEP\) and protein \(CSP\) containing](#)

503 [exopolymeric particles were in similar abundance at both stations. TEP and CSP were more](#)  
504 [abundant in the euphotic zone, which supports the idea of a phytoplankton origin; however, the](#)  
505 [concentration of TEP in this study was 69% \(in GB\) and 76% \(in LD\) lower than previously](#)  
506 reported for summer in the central Baltic Sea (Engel et al., 2002). Likewise, our dissolved  
507 inorganic nitrogen concentrations were below the detection limit in the surface, [while](#) phosphate  
508 concentrations were higher ( $>0.3 \mu\text{M}$ ) than [observed in the](#) Engel et al. (2002) study. Mari and  
509 Burd (1998) reported that TEP concentration peaked during the spring bloom and in summer in  
510 the Kattegat. TEP production may be enhanced by environmental conditions such as nutrient  
511 limitation (Mari et al., 2005; Passow, 2002), which are characteristic of late summer in the Baltic  
512 Sea (Mari and Burd 1998). [In the Baltic Sea, the spring bloom \(March-April\) is usually followed](#)  
513 [by a period of reduced PP \(Chl-\*a\*  \$\sim 2 \mu\text{gL}^{-1}\$ \) that preceded the cyanobacteria summer bloom,](#)  
514 [typically observed in June-July \(Kreus et al., 2015\).](#) Surface satellite-derived Chl-*a* concentrations  
515 (MODIS) in GB indicate [a constant increment from mid-May to mid-June 2015 \(Le Moigne et](#)  
516 [al., 2017\); our monthly Chl-\*a\* concentrations derived from VIIRS for June 2015 in the Baltic Sea](#)  
517 [\(Fig.1\) showed similar Chl-\*a\* concentrations. Considering this trend in Chl-\*a\* concentration and](#)  
518 [the availability of phosphate in the water column, we could assume that our samples were](#)  
519 [collected at the beginning of the summer bloom \(middle June\). In general ecosystem models from](#)  
520 [the Baltic Sea indicate that the termination of the summer bloom depends upon the phosphate](#)  
521 [availability \(Kreus et al., 2015\). Thus,](#) likely TEP concentrations had not reached the higher [value](#)  
522 [previously observed after summer bloom when inorganic nutrients were depleted-. Although](#)  
523 [satellite-derived Chl-\*a\* concentrations is a valuable tool to evaluate the trend of the PP, the](#)  
524 [magnitude of the concentration of Chl-\*a\* from remote sensing is difficult to estimate in the Baltic](#)  
525 [Sea \(Darecki and Stramski, 2004\). The concentration of Chl-\*a\* in GB and LD derived from direct](#)  
526 [measurements were much lower \( \$\sim 1.5 \mu\text{g L}^{-1}\$ \), suggesting that our samples were collected during](#)  
527 [a period of low phytoplankton biomass typically observed before the summer bloom. In any case,](#)  
528 [the concentration of phosphate was not limiting the system.](#) Another possible explanation for the  
529 rather low concentrations of TEP could be [their removal-](#) from the surface by aggregation and

530 subsequent sedimentation during the spring bloom due to the high abundance of cells and detrital  
531 particles during this time (Engel et al., 2002) [and the relatively low grazing pressure that lead to](#)  
532 [higher export after the spring bloom](#) (Lignell et al., 1993).

533 Although the composition and amount of OM in the surface waters at the two trap stations were  
534 similar, below the euphotic zone (40 m) the vertical profile of nutrients and [particulate matter](#)  
535 concentrations were [distinctly](#) different; likely due to the 2014/2015 MBI (Holtermann et al.,  
536 2017) that reached the deep waters of GB. This [inflow replaced the old stagnant water masses by](#)  
537 [new water masses \(Schmale et al., 2016\)](#), [changing](#) the salinity in the deepest waters and the  
538 vertical distribution of O<sub>2</sub> increasing its concentrations below 140 m and constraining the oxygen-  
539 deficient layers from 74 to 140 m depth. The combination of physical effects (the displacement of  
540 water masses, turbulent mixing and lateral transport) and the consequent development of redox  
541 conditions through 2015 may have impacted the distribution of MnOx-[like particles](#) and POM in  
542 GB. [In addition to changes in O<sub>2</sub> concentration, the MBI altered the redox conditions in GB](#)  
543 [creating a secondary redoxcline at 140 m, where concentrations of O<sub>2</sub> and MnOx-like particles](#)  
544 [increased. One consequence of those changes is the vertical extension of the layer in which](#)  
545 [MnOx-containing aggregates could form \(Schmale et al., 2016\); a previous study showed that](#)  
546 [MnOx might precipitate from the water column of GB following a MBI event \(Lenz et al., 2015\).](#)  
547 [POC and PN concentrations peaked at 110 m, this higher concentration at 110 m was even more](#)  
548 [evident in POP and TEP, while CSP concentration peaked at 140 m \(Fig. 3\); this is the first study](#)  
549 [that examines the potential role of CSP in forming aggregates with MnOx-containing particles.](#)  
550 [The highest concentration of MnO-like particles \(Fig. 4a\) in the water column was not observed at](#)  
551 [110 m \(the core of the OMZ\) but at 80 m \(oxycline\), and below 140 m in the newly oxygenated](#)  
552 [water layers.](#)

553 [In contrast, LD maintained permanent suboxic \(<5 μM O<sub>2</sub>\) waters below 74 m as H<sub>2</sub>S was](#)  
554 [detectable below 180 m. Below 100 m the vertical profiles of POM and BSi did not change with](#)  
555 [depth. The only exception was TEP and CSP concentration that similar to in GB peaked at 110 m](#)  
556 [and MnOx- like particles showed a small increment at 70 m \(in the oxycline\). This suggest that,](#)

557 [similar to the results of Glockzin et al \(2014\), the MnOx-like particles, abundant in the oxycline](#)  
558 [may form sinking aggregates with TEP and CSP, then, when those aggregates sunk to anoxic](#)  
559 [waters \(below 74 m\), the MnOx-like particles may dissolve releasing TEP and CSP to the water](#)  
560 [column, where CSP concentration decreased quickly likely due to microbial degradation, but the](#)  
561 [concentration of TEP remain constant to the bottom of LD.](#)

562 MBI can have a [significant](#) impact on nutrient recycling. In GB nitrate concentration increased  
563 possibly as a consequence of the oxidation of reduced nitrogen compounds (e.g., ammonium,  
564 ammonia and organic nitrogen compounds like urea) (Le Moigne et al., 2017) that accumulated  
565 during the stagnation (anoxic) period previous to the MBI (Hannig et al., 2007). [Scavenging of](#)  
566 [phosphate onto Mn or Fe oxides has been shown in previous studies \(Neretin et al., 2003\).](#)  
567 [Phosphate can](#) bind to [Fe](#) hydroxides and MnOx and settle down during oxic conditions, building  
568 up a phosphate pool in the sediments that later on when the O<sub>2</sub> decreases [may](#) become a source of  
569 phosphate (Gustafsson and Stigebrandt, 2007). Moreover, Myllykangas et al. (2017) reported that  
570 [the new water masses intruded during 2014/2015 MBI displaced the stagnant water masses in](#) GB.  
571 Thus, the low concentrations of silicate and phosphate that we measured in the deep waters of GB  
572 may also be a direct consequence of the intrusion of oxygenated, low-nutrient waters associated  
573 with the MBI. In contrast, in LD, the water column remained [anoxic down to](#) the sea floor (430  
574 m), below the oxycline an increase of ammonium was observed (Fig.2b), which could be an  
575 indicator for anaerobic respiration of OM, e.g., denitrification (Bonaglia et al., 2016; Hietanen et  
576 al., 2012).

577 In summary, though GB and LD had similar surface conditions in terms of phytoplankton  
578 production and POM stocks, during this study, we found differences [in the](#) vertical concentration  
579 of nutrients (Fig. 2) and POM (Fig. 3) [between](#) GB, ventilated by the MBI, [and](#) LD, a station that  
580 remained [suboxic](#). Our results suggest that [the MBI caused](#) differences in the vertical profile of O<sub>2</sub>  
581 [that modified](#) the redox conditions of the water column [and](#) enhance the [in-situ](#) formation of  
582 MnOx-like particles (Fig. 4). [Alternatively, the inflow may transport new MnOx-like particles to](#)

583 [GB. Those abundant MnOx-like particles](#) may aggregate with POM in GB, influencing the  
584 vertical distribution of POM in the water column.

585 *4.2 Potential influence of O<sub>2</sub> concentration and redox conditions on [vertical flux of sinking](#)*  
586 *[particles](#) in GB and LD*

587 During this study, we also investigated the effect of different O<sub>2</sub> concentrations and redox  
588 conditions on the fluxes of particles. Our measurement of [POC](#) flux at 40 m, below the euphotic  
589 zone, were 11.7±0.82 mmol C m<sup>-2</sup> d<sup>-1</sup> in GB and 19.8±1.22 mmol C m<sup>-2</sup> d<sup>-1</sup> in LD. Extrapolating  
590 those measurements to annual flux, we obtain 4.37±0.31 mol C m<sup>-2</sup> [yr](#)<sup>-1</sup> in GB and 7.44±0.46 mol  
591 C m<sup>-2</sup> yr<sup>-1</sup> in LD. Our results from [GB](#) are in the same range [as the estimation derived from a](#)  
592 [biogeochemical](#) model; *i.e.* 3.8 - 4.2 mol C m<sup>-2</sup> [yr](#)<sup>-1</sup> (Kreus et al., 2015; Sandberg et al., 2000;  
593 Stigebrandt, 1991) for the Baltic Sea; however, our results from [LD](#) are higher than the [annual](#)  
594 [POC](#) fluxes predicted by those models. [The high POC flux observed in this study is not surprising](#)  
595 [since it represented one \(in LD\) and two \(in GB\) days in June when the POC vertical flux out of](#)  
596 [the euphotic zone is relatively higher in the Baltic Sea compared with late fall and winter. The](#)  
597 [biogeochemical model of Kreis et al. \(personal communication\) estimated that POC flux in June](#)  
598 [ranged between 8 and 13 mmol m<sup>-2</sup>d<sup>-1</sup>; this is in the same range that our observations.](#)

599 [One of the main advantages of our sediment traps is that we can study the flux of sinking particles](#)  
600 [at various depths simultaneously \(i.e. higher vertical resolution\). Therefore, we measured the](#)  
601 [POM flux in oxic waters \(40 m and 60 \(55\) m\); at the core of the OMZ \(110 m\) at 180 m in both](#)  
602 [basins. Traps located a 180 m depth collected particles in sulfidic waters at LD and in recently](#)  
603 [oxygenated waters \(affected by the MBI\) in GB. The vertical flux of POM and BSi was different](#)  
604 [at the two studied basins; for example, POC flux was between 25 and 40% higher in the upper](#)  
605 [110 m of the LD than in GB \(even though the PP was 10% higher in GB\). However, the POC](#)  
606 [fluxes at 180 m \(deepest trap\) were similar in both basins; indicating a substantial decrease in](#)  
607 [the POC flux between 110 and 180 m at the LD. The POC flux \(and the PN flux which showed a](#)  
608 [similar vertical profile\) did not decrease with depth in the GB. In contrast, in the LD there was a](#)

609 reduction of 17 and 16% of the POC flux from 40 m and 60 m (in the oxycline) and from 110 to  
610 180 m respectively; the POC flux did not change from 60 to 110 m when a large section of the  
611 water column was suboxic ( $O_2 < 5 \mu\text{M}$  from 74 m to the bottom of the station). From 110 to 180  
612 m the water column was completely anoxic, and  $H_2S$  was detectable at 180 m. The high flux of  
613 POC at GB coincided with the appearance of dark, star-shaped particles that we defined as  
614 MnOx-like particles, particularly evident at GB (Fig. 6a,b, and e), but also present in LD. Based  
615 on their morphology, size, and aggregation with OM, we propose that those particles correspond  
616 to MnOx-containing particles enriched in OM that have been previously described at GB (Neretin  
617 et al., 2003; Pohl et al., 2004; Glockzin et al., 2014; Dellwig et al., 2010, 2018) and LD (Glockzin  
618 et al., 2014; Dellwig et al., 2010). The higher flux of MnOx-like particles in GB than in LD is  
619 probably due to the oxygenation and change in the deep water redox conditions that enhance the  
620 formation of MnOx-like particles associated with OM. This suggests that the reduction of the  
621 POC flux below 110 m in the LD may be related to the  $O_2$  depletion and the absence of MnOx-  
622 OM aggregates in the anoxic zone.

623 The POP flux was similar in the oxic water column (up to 60 m) in both basins; however, it was  
624 almost two and three times higher at 110 and 180 m respectively in GB than in LD. A peak in the  
625 POP and BSi flux was observed at 110 m in both basins, but the magnitude of the increment was  
626 much higher GB than in LD. In GB the POP flux increased 62% from 60 to 110 m (OMZ) and  
627 then decreased by 28% from 110 to 180 m. Vertical flux of POP, BSi, and Chl-*a* (Fig. 5) were  
628 enhanced at 110 m, which coincide with the high flux of MnOx-like particles. This high flux of  
629 MnOx-like particles is maintained at 180 m, while the POP, BSi and Chl-*a* flux decreased at this  
630 depth. This vertical distribution is likely due to the enhanced formation of MnOx-like particles  
631 in the hypoxic layer ( $<40 \mu\text{M } O_2$ ) located between 74 and 140 m that may scavenge POP, and  
632 aggregate with cells or phytodetritus containing BSi and Chl-*a*. Although the POP flux peaked at  
633 110 m in LD as well, the increment was only 30 % from 60 m (suboxic) to 110 m (anoxic), and it  
634 decreased by 78% from 110 to 180 m (sulfidic waters), these variations with depth were also

635 [observed in the BSi flux. In LD, the flux and size of MnOx-like particles were much smaller than](#)  
636 [in GB, and they were more abundant at 110 m than at 180 m.](#)

637 Similar to the vertical distribution [of POM](#) in the water column discussed in section [4.1](#),  
638 differences in POM [and BSi](#) fluxes between [basins](#) are likely associated with the large inflow of  
639 oxygen-rich saltwater that displaced the old-stagnant water masses and changed the chemistry of  
640 the water column (Myllykangas et al., 2017). Under euxinic conditions [\(e.i., scenario observed in](#)  
641 [LD without the influence of the MBI\)](#), the maximum concentration of particulate Mn is found [in](#)  
642 the oxycline (Glockzin et al., 2014). Below the oxycline, and due to [the presence of H<sub>2</sub>S](#), the  
643 particulate Mn concentration decreased drastically. During this study, we observed [a high](#)  
644 concentration of MnOx-[like](#) particles flux at 110 and 180 m (Table 5) in GB, [in agreement](#) with  
645 the high flux of particulate Mn measured in sediment traps located at 186 m in June 2015  
646 (Dellwig et al., 2018). The oxygenation of the deep water layers of GB by the MBI caused the  
647 absence of H<sub>2</sub>S (Schmale et al., 2016) and provided [-redox conditions favorable for the formation](#)  
648 [of MnOx, resulting in the high MnOx-like particles flux measured](#) in the sediment trap located in  
649 the core of the OMZ (110 m) and at 180 m [\(oxygenated deep water\)](#). There were two possible  
650 sources of MnOx associated with the 2014/2015 MBI [in GB](#). [On the](#) one hand, the lateral  
651 transport of low-density aggregates formed by MnOx and OM (Glockzin et al., 2014), and on the  
652 other hand, the *in-situ* formation and deposition of MnOx [following the oxygenation of the water](#)  
653 [column](#) (Dellwig et al., 2018). In clear contrast to the oxygenated deep layers of GB, in LD, we  
654 measured H<sub>2</sub>S [below](#) 180 m, this could explain why although those aggregates were present in  
655 this station at 110 m, they [may dissolve](#) in sulfidic waters, thus, were not as abundant and did not  
656 form aggregates with TEP (Fig.6c).

657 The presence of MnOx-[like particles in](#) aggregates (Fig 6a) may have implications for the vertical  
658 flux of [POC, PN](#) and [POP](#) in a stratified system with a pelagic redoxcline like the Baltic Sea.  
659 Under steady state, the upward diffusion and oxidation rates [of the dissolved Mn](#) are balanced by  
660 the sinking and dissolution rates [of MnOx](#). During Mn-oxidation, the [MnOx](#) could aggregate with  
661 [POM](#) and trace metals. Then, in the sulfidic waters, slow-sinking MnOx enriched in OM will be



662 dissolved liberating the OM and altering the vertical distribution and the flux of all associated  
663 particle elements (Glockzin et al., 2014). [This has been previously observed in other anoxic](#)  
664 [basins](#); for example, in the Cariaco Basin, total particulate phosphorus reached their maximum  
665 flux in sediment traps close to the redoxcline (Benitez-Nelson et al., 2004; Benitez-Nelson et al.,  
666 2007). Moreover, even in the anoxic zone, the abundant aggregate associated bacteria (Grossart et  
667 al., 2006) could partially or [entirely](#) degrade the organic compounds in those particles using  $\text{NO}_3^-$   
668 or MnOx as an electron acceptor. This may explain why we observed a clear peak in the [vertical](#)  
669 [fluxes](#) of POP, BSi, Chl-*a* (Fig. 3a, b), TEP (Fig. 6a) and TCHO (Fig. 7a) at 110 m, followed by a  
670 small decrease at 180 m in GB. In LD a smaller increment in the [vertical fluxes](#) of POP, BSi (Fig.  
671 3d), TEP (Fig. 6c) and TCHO (Fig. 7b) [were](#) also observed. The vertical fluxes of those  
672 compounds coincided with the abundance of MnOx-[like](#) particles; we assume that the MnOx  
673 aggregated not only with TEP as described before (Glockzin et al. 2014) and observed in this  
674 study (Fig. 6a), but-also with [aggregates containing phytoplankton cells and phytodetritus that](#)  
675 [may enhance](#) POP, BSi, Chl *a*, and TCHO [export](#). On the other hand, nitrogen-rich components of  
676 POM like PN (Fig. 3a), TAA (Fig. 7a), and CSP (Fig. 6a) gradually decreased with depth in GB,  
677 suggesting that those compounds were less scavenged by MnOx-OM rich aggregates.

678 [Primary production \(PP\)](#) in GB was 10% higher than in LD during our study (Piontek et al.  
679 unpublished data). However, the POC flux below the euphotic zone (at 40 m) was 42% higher in  
680 LD than in GB and comparable at both stations at 180 m. The fraction of PP exported as POC is  
681 termed export production (*e-ratio*) (Buesseler et al., 1992), and it is calculated as the POC flux  
682 below the euphotic zone divided by the [PP](#). [We calculated the](#) *e-ratio* using  $^{14}\text{C}$ -based PP  
683 [measurements](#) (Piontek et al. unpublished data) and carbon flux at 40 m (shallowest sediment trap  
684 depth, considered at the base of the euphotic zone). The *e-ratio* was [larger in LD \(0.77\) compared](#)  
685 [to GB \(0.41\)](#); *i.e.*, [the percentage of](#) the [PP](#) exported as POC below the euphotic zone [was](#) 77% in  
686 LD [versus 41% in GB](#). This suggests that either a higher proportion of the [PP](#) was remineralized  
687 in the euphotic zone of GB compared with LD, [or particles were sinking faster in LD than in GB](#)  
688 [likely due to differences in composition](#). On the other hand, the transfer efficiency of POC to the

689 deeper water column (*i.e.*, the ratio of POC flux at 180 m over POC flux at 40 m) was higher in  
690 GB (115%) than in LD (69%). The transfer efficiency of POM is largely controlled by the  
691 remineralization rate and the sinking velocity of particles (De La Rocha and Passow, 2007;  
692 McDonnell et al., 2015; Trull et al., 2008). The higher POC transfer efficiency in GB than in LD  
693 can be attributable to differences in the sinking velocities of the particles in those two stations.  
694 Particulate MnOx may sink through the redoxcline in GB (Neretin et al., 2003) acting as ballast  
695 material and nucleus for MnOx-OM rich aggregates formation. Those aggregates could have sunk  
696 more quickly, limiting the time spent in the water column and the degradation by particle-  
697 attached microbes. Assuming that MnOx-like particles had a density between 1.5 and 2.0 g cm<sup>-3</sup>  
698 (Glockzin et al., 2014), the largest particles measured at GB (167 μm, Table 4) will have a sinking  
699 velocity based on Stokes' law between 508 and 1014 m d<sup>-1</sup>. If we consider a mixed aggregate that  
700 is 50% TEP, density 0.9 g cm<sup>-3</sup> (Azetsu-Scott and Passow, 2004) and 50% MnOx (density 1.5 g  
701 cm<sup>-3</sup>), its density would be 1.2 g cm<sup>-3</sup>, and its theoretical sinking velocity will be 204 m d<sup>-1</sup>. This  
702 indicates that, theoretically, the largest mixed aggregates composed of MnOx and TEP observed  
703 in GB could reach 180 m (the location of our deepest sediment trap) in less than one day.  
704 However, the average measured sinking velocity of MnOx-containing particles in the laboratory  
705 for particles between 2 and 20 μm was 0.76 m d<sup>-1</sup>, which is significantly lower than the theoretical  
706 value (Glockzin et al., 2014). Glockzin et al. (2014) suggested that the star shape and the content  
707 of OM were responsible for the lower than predicted sinking velocity. There is no information  
708 about the amount of OM relatively to MnOx-containing particles in those mixed aggregates, or  
709 how the MnOx to OM ratio may affect the density and sinking velocity of larger aggregates like  
710 the ones we observed. Due to the shape and size of MnOx-OM aggregates observed in our study  
711 (Fig. 6e), we could assume those are the same type of aggregates described before by Glockzin et  
712 al. (2014). Although we did not measure the sinking velocity of those aggregates, we did observe  
713 a higher abundance of them associated with TEP at 110 and 180 m in GB than in LD. Thus, the  
714 formation of MnOx aggregates rich in OM could represent an additional mechanism (see  
715 introduction) to explain why the efficiency of the OM export is different under anoxic than under

716 oxic conditions in the Baltic Sea. The oxygenation of anoxic deep water in GB caused by the  
717 2014/2015 MBI, may have led to enhanced precipitation of manganese, iron, and phosphorus  
718 particles (Dellwig et al., 2010; Dellwig et al., 2018). For example, the formation of P-rich, metal  
719 oxides precipitates occur in the anoxic waters of the Black Sea (Shaffer, 1986) and Cariaco Basin  
720 (Benitez-Nelson et al., 2004; Benitez-Nelson et al., 2007) where higher concentration of particulate  
721 inorganic and organic phosphorus have been observed in sediment traps close to the redoxcline.

722 Alternatively, BSi could also act as ballast material incrementing the sinking velocity of marine  
723 aggregates (Armstrong et al., 2001; Klaas and Archer, 2002). Our results showed that sinking  
724 particles were strongly enriched in BSi relatively to C and N and compared to suspended particles  
725 that were depleted in BSi (Table 5). Diatoms are the major phytoplankton group that produces  
726 BSi to build their cell walls (Martin-Jézéquel et al., 2000), and they are the dominant  
727 phytoplankton species during the spring bloom. However, during our study, diatoms represented  
728 less than 1% of the phytoplankton abundance in the water column, and even though there was a  
729 strong enrichment in BSi in the sinking particles, this was similar in GB and LD (Table 5).  
730 Therefore, either the differences in export production nor in transfer efficiency between GB and  
731 LD could not be solely explained by the amount of diatoms cells, phytodetritus or BSi in sinking  
732 particles at those two basins.

#### 733 *4.3 Differences on composition and lability of sinking and suspended organic matter in GB and* 734 *LD*

735 In the sections above we compared the biogeochemical conditions and the size of the POM pool  
736 in the euphotic zone of GB and LD. We then looked at how the sinking flux of OM was affected  
737 by the different O<sub>2</sub> concentrations in the water column. Now, we focus on the influence of O<sub>2</sub> in  
738 the chemical composition of sinking and suspended particles. Suspended or slow sinking particles  
739 that spend more time in the water column should theoretically, show a more substantial degree of  
740 degradation (Goutx et al., 2007). Relative to the Redfield molar ratio: 106\_POC:16 PN: 15 BSi:  
741 POP. POM showed enrichment in POC relative to PN and POP, especially in sinking particles

742 from LD and suspended [particles](#) from GB. Our measured values of POC:PN (~10) and POC:POP  
743 (between 89 and 506) in suspended OM coincide with the simulated ratio reported immediately  
744 after the culmination of the spring bloom [by Kreuz et al. \(2015\)](#). The same study had suggested  
745 that POC:POP higher than Redfield ratio might lead to an enhancement of particle export (Kreuz  
746 et al., 2015), however, no direct observations had confirmed this hypothesis. Our measurements  
747 showed that the relative higher POC:POP ratios in sinking OM from LD, compared with GB, do  
748 not lead to a higher transfer efficiency at this station. Compared to the suspended OM in LD, the  
749 POP content was lower in GB, possible related to scavenging of POP into MnOx aggregates (see  
750 section 3.4).

751 [In addition, at both stations, sinking particles were strongly enriched in BSi \(Table 5\) probably](#)  
752 [due to the preferential sinking of diatoms and remnants diatom-rich detritus from the spring](#)  
753 [bloom. Differently, suspended particles had a relatively low content of BSi; this is not surprising](#)  
754 [considering the small proportions of diatoms in the euphotic zone at the time of our sampling. The](#)  
755 [concentration of BSi decreased below the detection limit from 60 m in the GB, and 70 m in the](#)  
756 [LD. This observation coincides with previous studies reporting selective incorporation of diatoms](#)  
757 [into sinking aggregates in the Baltic Sea \(Engel et al., 2002; Passow, 1991\), whereas non-diatoms](#)  
758 [species, although they may be abundant in the suspended phytoplankton, may not be present in](#)  
759 [sinking particles \(Passow, 1991\).](#)

760 [Another explanation for of higher BSi content in sinking particles may be the inclusion of](#)  
761 [lithogenic Si in our measurements; lithogenic Si may have been present in the water column or](#)  
762 [being transported by laterally advected material. A recent study suggests that contributions of non-](#)  
763 [biogenic sources could be significant during alkaline extraction \(Barão et al., 2015\). The even](#)  
764 [more substantial enrichment in BSi observed in sinking particles from 110 m in both basins, may](#)  
765 [result from adsorption and/or co-precipitation of silica in sinking particles containing MnOx](#)  
766 [\(Dellwig et al., 2010; Hartmann, 1985\); or by the formation of aggregates that are enriched in](#)  
767 [MnOx as well as in phytodetritus from diatom origin.](#)

768 The TAA based degradation index, DI (Dauwe et al. 1999) covers a wide range of alteration  
769 stages; the more negative the DI, the more degraded the samples, positive DI indicates fresh  
770 organic matter. In our study, the sediment trap material had a DI between 0.10 and 1.14, while  
771 suspended OM has a DI between -0.26 and -1.25 (Table 5). These values coincide with what  
772 reported earlier by Dauwe et al. (1999), and indicate that: first, the sinking particles collected in  
773 the sediment traps were less altered (they have a more positive DI) than the suspended OM  
774 collected in the Niskin bottle. Second, sinking particles from GB were fresher than the ones from  
775 LD, and the degradation stage increased with depth in both stations. The higher contribution of  
776 AA and CHO to the POC pool in sinking than in suspended OM and the AA- DI indicates that  
777 suspended OM was more degraded than sinking OM. The highest degree of degradation in  
778 suspended OM and sinking OM from LD may be the result of a long time that light suspended  
779 OM or slow sinking particles spend exposed to degradation in fully oxygenated surface waters  
780 than dense, fast sinking particles collected in sediment traps.

781 The higher abundance of aggregates, formed by a combination of MnOx-like particles and OM,  
782 observed at 110 and 180 m in GB could act as bacteria hot spots that combined with a higher O<sub>2</sub>  
783 concentration in GB may increase the microbial degradation on sinking particles collected in GB.  
784 However, the AA-DI, indicated that sinking OM was less altered, and therefore more labile than  
785 the sinking OM in LD. This implied that in addition to the higher transfer efficiency of POC in  
786 GB (see discussion above); the OM reaching the seafloor was fresher and less degraded. This  
787 supports the idea that mix aggregates composed by MnOx and OM may be larger and faster  
788 sinking than the previously described by Glockzin et al. (2014). This explanation is mostly  
789 speculative, and based on the observation of large mixed aggregates in the 110 and 180 m traps  
790 (Fig. 6, Table 4). However, as mention in the previous section, further work on directly  
791 determin<sup>ing</sup> sinking velocity is required to prove this hypothesis.

## 792 **Conclusion**

793 Fluxes and composition of sinking particles were different in two deep basins in the Baltic Sea:  
794 GB and LD during early summer 2015. The two stations had similar surface characteristics and  
795 POM stock; however, at depth, the vertical profile of [the POM concentration, as well as the](#)  
796 [vertical flux of sinking particles](#) was different, [likely related to differences in the O<sub>2</sub>](#)  
797 [concentration](#). The 2014/2015 MBI supplied oxygen-rich waters to GB transporting solid material  
798 from [shallower areas](#) and modifying the O<sub>2</sub> vertical profile and the redox conditions in the  
799 otherwise permanent suboxic deep waters. This event did not affect LD allowing [for the](#)  
800 [comparison of](#) POM fluxes and composition under two different O<sub>2</sub> concentrations with similar  
801 surface water conditions. Export efficiency (*e-ratio*) derived from *in-situ* PP measurements and  
802 POC flux derivate from sediment traps indicated higher export efficiency in LD than in GB.  
803 However, the transfer efficiency (POC flux at 180 m over POC flux at 40 m) suggested that under  
804 anoxic conditions found in LD, a smaller portion of the POC exported below the euphotic zone  
805 was transferred to 180 m than under oxygenated conditions present in GB. The MBI also transport  
806 solid Mn from shallower areas towards GB deep that may have contributed to the higher  
807 abundance of MnOx-OM in GB. Our results suggest that a new possible mechanism to explain the  
808 differences in the OM fluxes under different O<sub>2</sub> concentration could be the formation and  
809 prevalence of aggregates composed of MnOx and organic matter in GB. Those aggregates were  
810 significantly larger and more abundant in GB compared to LD where sulfidic waters constrained  
811 their presence. [Our results indicate that at GB not only a higher proportion of the POM leaving](#)  
812 [the euphotic zone reached our deepest sediment trap, but also that this POM was fresher and less](#)  
813 [degraded](#). We propose that after a MBI in GB, the aggregates containing MnOx-like particles and  
814 organic matter could have reached the sediments relatively fast and unaltered, scavenging not  
815 only phosphorus and TEP, as described previously, but also other compounds [like BSi, POP and](#)  
816 [CSP](#). [The higher fraction of sinking particles exported below the euphotic zone and reaching 180](#)  
817 [m in GB suggest that at this station a significant fraction of the POM could reach the sediments,](#)  
818 [50 m below our deepest sediment trap, relatively unaltered](#). The remineralization of [the](#) organic  
819 matter reaching the sediments may contribute to the quick re-establishment of anoxic conditions  
820 in the sediment-water interface in GB. The relevance of this process needs to be further

821 investigated in order to be included in O<sub>2</sub> budget and long-term predictions of the MBI impact in  
822 the O<sub>2</sub> and OM cycles.

### 823 **Author Contributions**

824 C.C.N. designed and performed the sediment trap work at sea, analyzed samples and wrote the  
825 manuscript. F.A.C.L.M, designed and performed the sediment trap work at sea and contributed to  
826 the writing of the manuscript. A.E designed and participated in the scientific program at sea and  
827 discussed and commented on the manuscript.

### 828 **Acknowledgements**

829 This research was supported by the DFG Collaborative Research Center 754 “Climate-  
830 Biogeochemistry Interactions in the Tropical Ocean” (to A.E., C.C.N. and F.A.C.L.M), by a  
831 Fellowship of the Excellence Cluster ‘The Future Ocean’ (CP1403 to F.A.C.L.M.), and by a  
832 DAAD short term grant (57130097 to C.C.N.). We thank Jon Roa, Tania Klüver, Scarlett Sett,  
833 Angela Stippkugel, Carola Wagner, Clarissa Karthäuser, Moritz Ehrlich, Sonja Endres, Hannes  
834 Wagner, Ruth Flerus, Sven Sturm and Christian Begler for support during traps preparation and  
835 deployments, help with experiment or analyzed samples. We Thank Judith Piontek for her  
836 contribution to the design of the scientific program at sea, Jaime Soto- Neira for useful discussion  
837 and help with figure preparation and Cindy Lee for helpful advices.

## References

- Andersen, J. H., Carstensen, J., Conley, D. J., Dromph, K., Fleming-Lehtinen, V., Gustafsson, B. G., Josefson, A. B., Norkko, A., Villnäs, A., and Murray, C.: Long-term temporal and spatial trends in eutrophication status of the Baltic Sea, *Biological Reviews*, 92, 135-149, 2017.
- Armstrong, R. A., Lee, C., Hedges, J. I., Honjo, S., and Wakeham, S. G.: A new, mechanistic model for organic carbon fluxes in the ocean based on the quantitative association of POC with ballast minerals, *Deep Sea Research Part II: Topical Studies in Oceanography*, 49, 219-236, 2002.
- Azetsu-Scott, K. and Passow, U.: Ascending marine particles: Significance of transparent exopolymer particles (TEP) in the upper ocean, *Limnology and Oceanography*, 49, 741-748, 2004.
- Barão, L., Vandevenne, F., Clymans, W., Frings, P., Ragueneau, O., Meire, P., Conley, D. J., and Struyf, E.: Alkaline-extractable silicon from land to ocean: A challenge for biogenic silicon determination, *Limnology and Oceanography: Methods*, 13, 329-344, 2015.
- Benitez-Nelson, C. R., O'Neill, L., Kolowitz, L. C., Pellechia, P., and Thunel, I. R.: Phosphonates and particulate organic phosphorus cycling in an anoxic marine basin, *Limnology and Oceanography*, 49, 1593-1604, 2004.
- Benitez-Nelson, C. R., O'Neill Madden, L. P., Styles, R. M., Thunell, R. C., and Astor, Y.: Inorganic and organic sinking particulate phosphorus fluxes across the oxic/anoxic water column of Cariaco Basin, Venezuela, *Marine Chemistry*, 105, 90-100, 2007.
- Bianchi, T. S., Engelhaupt, E., Westman, P., Andrén, T., Rolff, C., and Elmgren, R.: Cyanobacterial blooms in the Baltic Sea: Natural or human-induced?, *Limnology and Oceanography*, 45, 716-726, 2000.
- Bonaglia, S., Klawonn, I., Brabandere, L. D., Deutsch, B., Thamdrup, B., and Brüchert, V.: Denitrification and DNRA at the Baltic Sea oxic–anoxic interface: Substrate spectrum and kinetics, *Limnology and Oceanography*, 61, 1900-1915, 2016.
- Boyd, P. W. and Trull, T. W.: Understanding the export of biogenic particles in oceanic waters: Is there consensus?, *Progress in Oceanography*, 72, 276-312, 2007.
- Bradford, M. M.: A rapid and sensitive method for the quantitation of microgram quantities of protein utilizing the principle of protein-dye binding, *Analytical Biochemistry*, 72, 248-254, 1976.
- Brettar, I. and Rheinheimer, G.: Denitrification in the Central Baltic: evidence for  $\text{H}_2\text{S}$  oxidation as motor of denitrification at the oxic-anoxic interface, *Marine Ecology Progress Series*, 77, 157-169, 1991.
- Buesseler, K. O., Antia, A. N., Chen, M., Fowler, S. W., Gardner, W. D., Gustafsson, Ö., Harada, K., Michaels, A. F., Rutgers v. d. Loeff, M., Sarin, M., Steinberg, D. K., and Trull, T. W.: An assessment of the use of sediment traps for estimating upper ocean particle fluxes, *Journal of Marine Research*, 65, 345-416, 2007.
- Buesseler, K. O., Bacon, M. P., Kirk Cochran, J., and Livingston, H. D.: Carbon and nitrogen export during the JGOFS North Atlantic Bloom experiment estimated from  $^{234}\text{Th}$ :  $^{238}\text{U}$  disequilibria, *Deep Sea Research Part A. Oceanographic Research Papers*, 39, 1115-1137, 1992.
- Carstensen, J., Andersen, J. H., Gustafsson, B. G., and Conley, D. J.: Deoxygenation of the Baltic Sea during the last century, *Proceedings of the National Academy of Sciences*, 111, 5628-5633, 2014a.
- Carstensen, J., Conley, D. J., Bonsdorff, E., Gustafsson, B. G., Hietanen, S., Janas, U., Jilbert, T., Maximov, A., Norkko, A., Norkko, J., Reed, D. C., Slomp, C. P., Timmermann, K., and Voss, M.: Hypoxia in the Baltic Sea: Biogeochemical Cycles, Benthic Fauna, and Management, *AMBIO*, 43, 26-36, 2014b.
- Cavan, E. L., Trimmer, M., Shelley, F., and Sanders, R.: Remineralization of particulate organic carbon in an ocean oxygen minimum zone, *Nature Communications*, 8, 14847, 2017.
- Cisternas-Nova, C., Lee, C., and Engel, A.: A semi-quantitative spectrophotometric, dye-binding assay for determination of Coomassie Blue stainable particles, *Limnology and Oceanography: Methods*, 12, 604-616, 2014.



Conley, D. J., Björck, S., Bonsdorff, E., Carstensen, J., Destouni, G., Gustafsson, B. G., Hietanen, S., Kortekaas, M., Kuosa, H., Markus Meier, H. E., Müller-Karulis, B., Nordberg, K., Norkko, A., Nürnberg, G., Pitkänen, H., Rabalais, N. N., Rosenberg, R., Savchuk, O. P., Slomp, C. P., Voss, M., Wulff, F., and Zillén, L.: Hypoxia-Related Processes in the Baltic Sea, *Environmental Science & Technology*, 43, 3412-3420, 2009.

Conte, M. H., Ralph, N., and Ross, E. H.: Seasonal and interannual variability in deep ocean particle fluxes at the Oceanic Flux Program (OFP)/Bermuda Atlantic Time Series (BATS) site in the western Sargasso Sea near Bermuda, *Deep Sea Research Part II: Topical Studies in Oceanography*, 48, 1471-1505, 2001.

Darecki, M. and Stramski, D.: An evaluation of MODIS and SeaWiFS bio-optical algorithms in the Baltic Sea, *Remote Sensing of Environment*, 89, 326-350, 2004.

Dauwe, B., Middelburg, J. J., Herman, P. M. J., and Heip, C. H. R.: Linking diagenetic alteration of amino acids and bulk organic matter reactivity, *Limnology and Oceanography*, 44, 1809-1814, 1999.

De La Rocha, C. L. and Passow, U.: Factors influencing the sinking of POC and the efficiency of the biological carbon pump, *Deep Sea Research Part II: Topical Studies in Oceanography*, 54, 639-658, 2007.

Dellwig, O., Leipe, T., März, C., Glockzin, M., Pollehne, F., Schnetger, B., Yakushev, E. V., Böttcher, M. E., and Brumsack, H.-J.: A new particulate Mn–Fe–P-shuttle at the redoxcline of anoxic basins, *Geochimica et Cosmochimica Acta*, 74, 7100-7115, 2010.

Dellwig, O., Schnetger, B., Brumsack, H.-J., Grossart, H.-P., and Umlauf, L.: Dissolved reactive manganese at pelagic redoxclines (part II): Hydrodynamic conditions for accumulation, *Journal of Marine Systems*, 90, 31-41, 2012.

Dellwig, O., Schnetger, B., Meyer, D., Pollehne, F., Häusler, K., and Arz, H. W.: Impact of the Major Baltic Inflow in 2014 on Manganese Cycling in the Gotland Deep (Baltic Sea), *Frontiers in Marine Science*, 5, 2018.

Devol, A. H. and Hartnett, H. E.: Role of the oxygen-deficient zone in transfer of organic carbon to the deep ocean, *Limnology and Oceanography*, 46, 1684-1690, 2001.

Dittmar, T., Cherrier, J., and Ludwichowski, K. U.: The analysis of amino acids in seawater. In: *Practical guidelines for the analysis of seawater* Wurl, O. and Raton, B. (Eds.), CRC Press, 2009.

Dollhopf, M. E., Nealson, K. H., Simon, D. M., and Luther, G. W.: Kinetics of Fe(III) and Mn(IV) reduction by the Black Sea strain of *Shewanella putrefaciens* using in situ solid state voltammetric Au/Hg electrodes, *Marine Chemistry*, 70, 171-180, 2000.

Dugdale, R. C. and Goering, J. J.: Uptake Of New And Regenerated Forms Of Nitrogen In Primary Productivity, *Limnology and Oceanography*, 12, 196-206, 1967.

Emeis, K. C., Struck, U., Leipe, T., Pollehne, F., Kunzendorf, H., and Christiansen, C.: Changes in the C, N, P burial rates in some Baltic Sea sediments over the last 150 years—relevance to P regeneration rates and the phosphorus cycle, *Marine Geology*, 167, 43-59, 2000.

Engel, A.: The role of transparent exopolymer particles (TEP) in the increase in apparent particle stickiness ( $\alpha$ ) during the decline of a diatom bloom, *Journal of Plankton Research*, 22, 485-497, 2000.

Engel, A., Meyerhöfer, M., and von Bröckel, K.: Chemical and Biological Composition of Suspended Particles and Aggregates in the Baltic Sea in Summer (1999), *Estuarine, Coastal and Shelf Science*, 55, 729-741, 2002.

Engel, A. and Schartau, M.: Influence of transparent exopolymer particles (TEP) on sinking velocity of *Nitzschia closterium* aggregates, *Marine Ecology Progress Series*, 182, 69-76, 1999.

Engel, A., Wagner, H., Le Moigne, F. A. C., and Wilson, S. T.: Particle export fluxes to the oxygen minimum zone of the eastern tropical North Atlantic, *Biogeosciences*, 14, 1825-1838, 2017.

Eppley, R. W. and Peterson, B. J.: Particulate organic matter flux and planktonic new production in the deep ocean, *Nature*, 282, 677, 1979.

Glockzin, M., Pollehne, F., and Dellwig, O.: Stationary sinking velocity of authigenic manganese oxides at pelagic redoxclines, *Marine Chemistry*, 160, 67-74, 2014.

Goutx, M., Wakeham, S. G., Lee, C., Duflo, s. M., Guigue, C., Liu, Z., Moriceau, B., Sempère, R., Tedetti, M., and Xue, J.: Composition and degradation of marine particles with different settling velocities in the northwestern Mediterranean Sea, *Limnology and Oceanography*, 52, 1645-1664, 2007.

Grossart, H. P., KiÅfÅrboe, T., Tang, K. W., Allgaier, M., Yam, E. M., and Ploug, H.: Interactions between marine snow and heterotrophic bacteria: aggregate formation and microbial dynamics, *Aquatic Microbial Ecology*, 42, 19-26, 2006.

Gustafsson, B. G. and Stigebrandt, A.: Dynamics of nutrients and oxygen/hydrogen sulfide in the Baltic Sea deep water, *Journal of Geophysical Research: Biogeosciences*, 112, 2007.

Hannig, M., Lavik, G., Kuypers, M. M. M., Woebken, D., Martens-Habbena, W., and Jürgens, K.: Shift from denitrification to anammox after inflow events in the central Baltic Sea, *Limnology and Oceanography*, 52, 1336-1345, 2007.

Hansen, H. P. and Koroleff, F.: Determination of nutrients. In: *Methods of Seawater Analysis*, Wiley-VCH Verlag GmbH, 2007.

Hansen, H. P. and Koroleff, F.: Determination of nutrients. In: *Methods of Seawater Analysis.*, Grasshoff, K., Kremling, K., and Ehrhardt, M. (Eds.), Wiley-VCH, Weinheim, Germany, 1999.

Hartmann, M.: Atlantis-II Deep geothermal brine system. Chemical processes between hydrothermal brines and Red Sea deep water, *Marine Geology*, 64, 157-177, 1985.

HELCOM: Guidelines for monitoring phytoplankton species composition, abundance and biomass. In: *Manual for Marine Monitoring in the COMBINE*

Programme of HELCOM, Helsinki Commission, Helsinki 2012.

Hietanen, S., Jäntti, H., Buizert, C., Jürgens, K., Labrenz, M., Voss, M., and Kuparinen, J.: Hypoxia and nitrogen processing in the Baltic Sea water column, *Limnology and Oceanography*, 57, 325-337, 2012.

Holtermann, P. L., Prien, R., Naumann, M., Mohrholz, V., and Umlauf, L.: Deepwater dynamics and mixing processes during a major inflow event in the central Baltic Sea, *Journal of Geophysical Research: Oceans*, 122, 6648-6667, 2017.

Keil, R. G., Neibauer, J. A., Biladeau, C., van der Elst, K., and Devol, A. H.: A multiproxy approach to understanding the "enhanced" flux of organic matter through the oxygen-deficient waters of the Arabian Sea, *Biogeosciences*, 13, 2077-2092, 2016.

Knauer, G. A., Martin, J. H., and Bruland, K. W.: Fluxes of particulate carbon, nitrogen, and phosphorus in the upper water column of the northeast Pacific, *Deep Sea Research Part A. Oceanographic Research Papers*, 26, 97-108, 1979.

Kreus, M., Schartau, M., Engel, A., Nausch, M., and Voss, M.: Variations in the elemental ratio of organic matter in the central Baltic Sea: Part I—Linking primary production to remineralization, *Continental Shelf Research*, 100, 25-45, 2015.

Kullenberg, G. and Jacobsen, T. S.: The Baltic Sea: an outline of its physical oceanography, *Marine Pollution Bulletin*, 12, 183-186, 1981.

Le Moigne, F. A. C., Cisternas-Novoa, C., Piontek, J., Maßmig, M., and Engel, A.: On the effect of low oxygen concentrations on bacterial degradation of sinking particles, *Scientific Reports*, 7, 16722, 2017.

Legendre, L. and Gosselin, M.: New production and export of organic matter to the deep ocean: Consequences of some recent discoveries, *Limnology and Oceanography*, 34, 1374-1380, 1989.

Leipe, T., Tauber, F., Vallius, H., Virtasalo, J., Uścińowicz, S., Kowalski, N., Hille, S., Lindgren, S., and Myllyvirta, T.: Particulate organic carbon (POC) in surface sediments of the Baltic Sea, *Geo-Marine Letters*, 31, 175-188, 2011.

Lenz, C., Jilbert, T., Conley, D. J., Wolthers, M., and Slomp, C. P.: Are recent changes in sediment manganese sequestration in the euxinic basins of the Baltic Sea linked to the expansion of hypoxia?, *Biogeosciences*, 12, 4875-4894, 2015.

Lignell, R. R., Heiskanen, A.-S., Kuosa, H., Kuuppo-Leinikki, P., Pajuniemi, R., and Uitto, A.: Fate of phytoplankton spring bloom: Sedimentation and carbon flow in the planktonic food web in the northern Baltic, *Marine Ecology. Progress Series*, 94, 13, 1993.

Lindroth, P. and Mopper, K.: High performance liquid chromatographic determination of subpicomole amounts of amino acids by precolumn fluorescence derivatization with o-phthalaldehyde, *Analytical Chemistry*, 51, 1667-1674, 1979.

Logan, B. E., Passow, U., Alldredge, A. L., Grossartt, H.-P., and Simont, M.: Rapid formation and sedimentation of large aggregates is predictable from coagulation rates (half-lives) of transparent exopolymer particles (TEP), *Deep Sea Research Part II: Topical Studies in Oceanography*, 42, 203-214, 1995.

Mari, X. and Burd, A.: Seasonal size spectra of transparent exopolymeric particles (TEP) in a coastal sea and comparison with those predicted using coagulation theory, *Marine Ecology Progress Series*, 163, 13, 1998.

Mari, X., Rassoulzadegan, F., Brussaard, C. P. D., and Wassmann, P.: Dynamics of transparent exopolymeric particles (TEP) production by *Phaeocystis globosa* under N- or P-limitation: a controlling factor of the retention/export balance, *Harmful Algae*, 4, 895-914, 2005.

Martin-Jézéquel, V., Hildebrand, M., and Brzezinski, M. A.: SILICON METABOLISM IN DIATOMS: IMPLICATIONS FOR GROWTH *Journal of Phycology*, 36, 821-840, 2000.

Matthäus, W. and Franck, H.: Characteristics of major Baltic inflows—a statistical analysis, *Continental Shelf Research*, 12, 1375-1400, 1992.

McDonnell, A. M. P., Boyd, P. W., and Buesseler, K. O.: Effects of sinking velocities and microbial respiration rates on the attenuation of particulate carbon fluxes through the mesopelagic zone, *Global Biogeochemical Cycles*, 29, 175-193, 2015.

Myllykangas, J. P., Jilbert, T., Jakobs, G., Rehder, G., Werner, J., and Hietanen, S.: Effects of the 2014 major Baltic inflow on methane and nitrous oxide dynamics in the water column of the central Baltic Sea, *Earth Syst. Dynam.*, 8, 817-826, 2017.

Nausch, M., Nausch, G., Lass, H. U., Mohrholz, V., Nagel, K., Siegel, H., and Wasmund, N.: Phosphorus input by upwelling in the eastern Gotland Basin (Baltic Sea) in summer and its effects on filamentous cyanobacteria, *Estuarine, Coastal and Shelf Science*, 83, 434-442, 2009.

Neretin, L. N., Pohl, C., Jost, G., Leipe, T., and Pollehne, F.: Manganese cycling in the Gotland Deep, Baltic Sea, *Marine Chemistry*, 82, 125-143, 2003.

Passow, U.: Production of transparent exopolymer particles (TEP) by phyto- and bacterioplankton, *Marine Ecology Progress Series*, 236, 12, 2002.

Passow, U.: Species-specific sedimentation and sinking velocities of diatoms, *Marine Biology*, 108, 449-455, 1991.

Passow, U. and Alldredge, A. L.: A dye-binding assay for the spectrophotometric measurement of transparent exopolymer particles (TEP), *Limnology and Oceanography*, 40, 1326-1335, 1995.

Richardson, L. L., Aguilar, C., and Neilson, K. H.: Manganese oxidation in pH and O<sub>2</sub> microenvironments produced by phytoplankton<sup>1,2</sup>, *Limnology and Oceanography*, 33, 352-363, 1988.

Sandberg, J., Elmgren, R., and Wulff, F.: Carbon flows in Baltic Sea food webs — a re-evaluation using a mass balance approach, *Journal of Marine Systems*, 25, 249-260, 2000.

Schmale, O., Krause, S., Holtermann, P., Power Guerra, N. C., and Umlauf, L.: Dense bottom gravity currents and their impact on pelagic methanotrophy at oxic/anoxic transition zones, *Geophysical Research Letters*, 43, 5225-5232, 2016.

Shaffer, G.: Phosphate pumps and shuttles in the Black Sea, *Nature*, 321, 515, 1986.

Stigebrandt, A.: Computations of oxygen fluxes through the sea surface and the net production of organic matter with application to the Baltic and adjacent seas, *Limnology and Oceanography*, 36, 444-454, 1991.

Strickland, J. D. and Parsons, T. R.: Determination of dissolved oxygen. In: *A Practical Handbook of Seawater Analysis*, Fisheries Research Board of Canada, 1968.

Strickland, J. D. H., Parsons, T. R., and Strickland, J. D. H.: A practical handbook of seawater analysis, Fisheries Research Board of Canada, Ottawa, 1972.

Thomas, H. and Schneider, B.: The seasonal cycle of carbon dioxide in Baltic Sea surface waters, *Journal of Marine Systems*, 22, 53-67, 1999.

Thornton, D. C. O.: Coomassie Stainable Particles (CSP): Protein Containing Exopolymer Particles in the Ocean, *Frontiers in Marine Science*, 5, 2018.

Trull, T. W., Bray, S. G., Buesseler, K. O., Lamborg, C. H., Manganini, S., Moy, C., and Valdes, J.: In situ measurement of mesopelagic particle sinking rates and the control of carbon transfer to the ocean interior during the Vertical Flux in the Global Ocean (VERTIGO) voyages in the North Pacific, *Deep Sea Research Part II: Topical Studies in Oceanography*, 55, 1684-1695, 2008.

Turner, J. T.: Zooplankton fecal pellets, marine snow, phytodetritus and the ocean's biological pump, *Progress in Oceanography*, 130, 205-248, 2015.

van Hulst, M., Middag, R., Dutay, J. C., de Baar, H., Roy-Barman, M., Gehlen, M., Tagliabue, A., and Sterl, A.: Manganese in the west Atlantic Ocean in the context of the first global ocean circulation model of manganese, *Biogeosciences*, 14, 1123-1152, 2017.

Van Mooy, B. A. S., Keil, R. G., and Devol, A. H.: Impact of suboxia on sinking particulate organic carbon: Enhanced carbon flux and preferential degradation of amino acids via denitrification, *Geochimica et Cosmochimica Acta*, 66, 457-465, 2002.

Wasmund, N.: Occurrence of cyanobacterial blooms in the Baltic sea in relation to environmental conditions, *Internationale Revue der gesamten Hydrobiologie und Hydrographie*, 82, 169-184, 1997.

Wasmund, N. and Uhlig, S.: Phytoplankton trends in the Baltic Sea, *ICES Journal of Marine Science*, 60, 2003.

Wilhelm, W. L.: Die Bestimmung des im Wasser gelösten Sauerstoffes, *Berichte der deutschen chemischen Gesellschaft*, 21, 2843-2854, 1888.

## Figure Captions

Figure 1. Monthly averaged Chl *a* distribution derived from VIIRS for June 2015 in the Baltic Sea.

Black circle and “x” - indicate the position of the trap deployment and the seawater collection, respectively, in Gotland Deep (GB) and Landsort Deep (LD). The lower panel shows the trajectory of the trap deployed at GB and LD.

Figure 2. Water column profiles at the location of the sediment trap deployments in (A) GB, and (B)

LD. Left panel: oxygen (blue), temperature (red), and salinity (black). Middle panel: nitrate (NO<sub>3</sub>, [white squares](#)), nitrite (NO<sub>2</sub>, [grey circles](#)), and ammonium (NH<sub>4</sub>, [black triangles](#)). Right panel: phosphate (PO<sub>4</sub>, [grey diamond](#)), and silicate (Si(OH)<sub>4</sub>, [black circles](#)). Grey lines indicate the depths at which we deployed sediment traps.

Figure 3. [Vertical profiles of concentration of](#) particulate organic carbon (POC), particulate nitrogen (PN), [and](#) particulate organic phosphorus (POP) [in GB \(A\) and LD \(D\); vertical profiles of](#) [concentration of](#) chlorophyll *a* (Chl *a*) and biogenic silicate (BSi) [in GB \(B\) and LD \(D\); and vertical profiles of concentration of](#) transparent exopolymeric particles (TEP) and Coomassie stainable particles (CSP) [in GB \(C\) and LD \(F\)](#) Grey lines as figure 2.

Figure 4. [Vertical profiles of](#) MnOx-like particles and O<sub>2</sub> concentration in the water column at the location of the sediment traps deployments. (A) GB and (B) LD. Grey lines as in figure 3.

Figure 5. [Vertical fluxes of particulate organic carbon \(POC\) and particulate nitrogen \(PN\) as well as oxygen concentration](#) in GB (A) [and LD \(C\)](#). [Vertical fluxes of particulate organic phosphorus \(POP\), biogenic silica \(BSi\) and chlorophyll \*a\* \(Chl \*a\*\)](#) in GB (B) [and LD \(D\)](#).

Figure 6. TEP and CSP fluxes in GB (A and B) and LD (C and D). In addition to vertical fluxes, each profile is complemented with [microscopic](#) images (200x) [of material collected at](#) each depth. [In GB,](#) star-shaped MnOx-like particles are clearly visible [as single particles and forming aggregates with](#) TEP (A), [and](#) CSP (B). MnOx-like particles were less abundant in LD (C and D). (F) A larger magnification (400x) image of MnOx-like particles at 110 m showing more detail on the shape of those particles and aggregates formed with TEP.

Figure 7. [Vertical fluxes of](#) total hydrolyzable amino acids (TAA) and total carbohydrates (TCHO) [as well as oxygen concentration in](#) (A) GB, and (B) LD.

Table 1. Sediment traps deployment and recovery locations, dates, collection times and depths. [Two sediment traps were deployed at 40 m \(A and B\) to evaluate replicability.](#)

Station	Lat	Lon	Date	Station depth	Deployment time (d)	Trap depths (m)
Gotland Basin (GB)	57.21 °N	20.03 °E	08/06/2015	248 m	2	40A, 40B, 60, 110, and 180m
	57.27 °N	20.25 °E	10/06/2015			
Landsort Deep (LD)	58.69 °N	18.55 °E	15/06/2015	460 m	1	40A, 40B, 55, 110, and 180m
	58.68 °N	18.68 °E	16/06/2015			

Table 2. Abundance of chlorophyll and phycoerythrin containing pico- and nano-plankton measured by [flow cytometry](#) in GB and LD.

	Depth (m)	Phytoplankton (cells mL <sup>-1</sup> )			Cyanobacteria-like (cells mL <sup>-1</sup> )		
		picoplankton	nanoplankton	Total	picoplankton	nanoplankton	Total
GB	1	87963	2097	90060	5225	731	5956
	10	94369	2628	96997	8795	920	9716
	40	4999	68	5067	2174	69	2243
	60	4125	35	4160	1990	42	2032
	80	599	7	606	238	15	253
	110	594	7	601	326	29	356
	140	1144	14	1158	356	2	358
	180	908	9	917	366	20	385
	220	2270	19	2289	1063	34	1097
LD	1	92359	2283	94642	834	177	1011
	10	86426	1708	88134	2990	232	3223
	40	2022	92	2114	2243	69	2312
	60	1524	62	1586	1294	24	1318
	70	908	43	951	613	17	630
	110	1735	82	1817	1181	17	1198
	180	1339	75	1415	946	34	980
	250	1593	82	1676	949	36	985
	300	1521	48	1569	1047	17	1064
	350	1608	57	1665	908	12	920
	400	1548	73	1621	1047	22	1069
	430	1562	68	1631	875	19	894



Table 3. Phytoplankton abundance analyzed microscopically [for samples collected at the location of trap deployment](#) in GB and LD.

		Phytoplankton Abundance (L <sup>-1</sup> )							
		GB				LD			
		1 m	10 m	40 m	Total	1 m	10 m	40 m	Total
Cyanobacteria*	Total	14148	13536	0	27684	37368	32526	96	69990
Chryptophyta	Total	140	112	28	280	1400	882	56	2338
Bacillariophyceae	Total	96	94	44	234	462	112	102	676
	<i>Chaetoceros</i> sp.	58	42	24	124	434	106	26	566
	<i>Skeletonema</i> sp.	26	8	12	46	12	0	8	20
	<i>Thalassiosira</i> sp.	12	44	8	64	16	6	68	90
Dinophyceae**	Total	3772	4424	1192	9388	9032	7662	1404	18098
	<i>Dinophysis</i> sp.	678	742	2	1422	450	214	4	668
	other	3094	3682	1190	7966	8582	7448	1400	17430
Chlorophyta	Total	5320	6860	28	12208	2072	1022	238	3332
	<i>Planctonema</i> sp.	5320	6860	28	12208	2072	1022	238	3332

[\\*Filamentous cyanobacteria were counted in 50 µm length units \(>90% were -\*Aphanizomenon\* sp.\)](#)

[\\*\\*Include mixotrophs](#)

Table 4. MnOx-like particle fluxes and size [as equivalent spherical diameter \(ESD\)](#) determined by image analysis in GB and LD.

Station	Depth (m)	MnOx-like particles (cm <sup>2</sup> m <sup>-2</sup> d <sup>-1</sup> )	Median size ESD (μm)	Size range ESD (μm)
GB	110	5666± 994	2.8	0.6-167
	180	7789± 955	3.3	0.6-153
LD	110	50.3±1.8	1.8	0.6-16.5
	180	2.6±0.3	1.4	1.2-9.3

Table 5. Amino acids (AA), carbohydrates (CHO), elemental molar ratios and amino acid-based degradation index of sinking and suspended [particles](#) in GB and in LD.

		Depth (m)	AA-C:POC %	CHO-C:POC %	POC:PN	POC:POP	POC:BSi	PN:BSi	PN:POP	DI
Sinking particles	GB	40	19.2	18.3	9.8	244	3.9	0.4	24.9	1.49
		40	17.6	17.2	9.4	222	4.1	0.4	23.6	1.43
		60	15.8	17.6	9.5	232	2.8	0.3	24.3	1.13
		110	13.9	22.2	11.3	90.1	1.7	0.2	8.0	0.71
		180	11.1	18.5	12.7	123	3.0	0.2	9.7	-0.03
	LD	40	13.5	9.4	12.2	772	3.6	0.3	63.4	0.30
		40	14.3	8.4	11.1	413	4.1	0.4	37.2	0.27
		55	19.1	11.0	12.4	332	3.0	0.2	26.7	-0.02
		110	13.4	12.0	15.4	230	2.7	0.2	14.9	0.11
		180	14.3	12.9	15.3	341	4.2	0.3	22.3	-0.29
Suspended particles	GB	1	8.2	16.9	10.4	155	91.4	8.8	14.9	
		10	10.8	8.8	10.5	151	87.1	8.3	14.4	
		40	4.9	2.8	9.2	88.8	134	15	9.7	-0.81
		60	5.4	2.7	9.8	127	125	13	13.0	-0.27
		80	4.7	0.00	10.4	145			13.9	
		110	9.0	6.6	8.5	245			29.0	0.98
		140	5.3	0.00	10.6	283			26.7	
		180	5.7	4.3	11.4	506			44.5	-0.40
	220	8.6	3.3	12.1	271			22.5		
	LD	1	7.0	0.00	8.7	205	515	59.5	23.7	
		10	13.0	9.1	8.4	196	101	12.0	23.3	
		40	0.00	8.9	8.1	336	24.5	3.0	41.5	-0.53
		60	6.1	10.3	7.8	301	16.9	2.2	38.4	-0.12
		70	7.9	10.7	7.7	292	248	32.1	37.9	
110		12.2	5.4	7.9	225			28.3	0.80	

180	10.1	11.3	7.0	205	29.2	0.34
250	12.0	8.8	6.5	249	38.2	
300	10.9	0.00	6.7	137	20.4	
350	10.7	10.1	6.8	146	21.6	
400	10.0	0.00	6.2	230	37.2	
430	9.4	9.5	7.8	149	19.0	

---

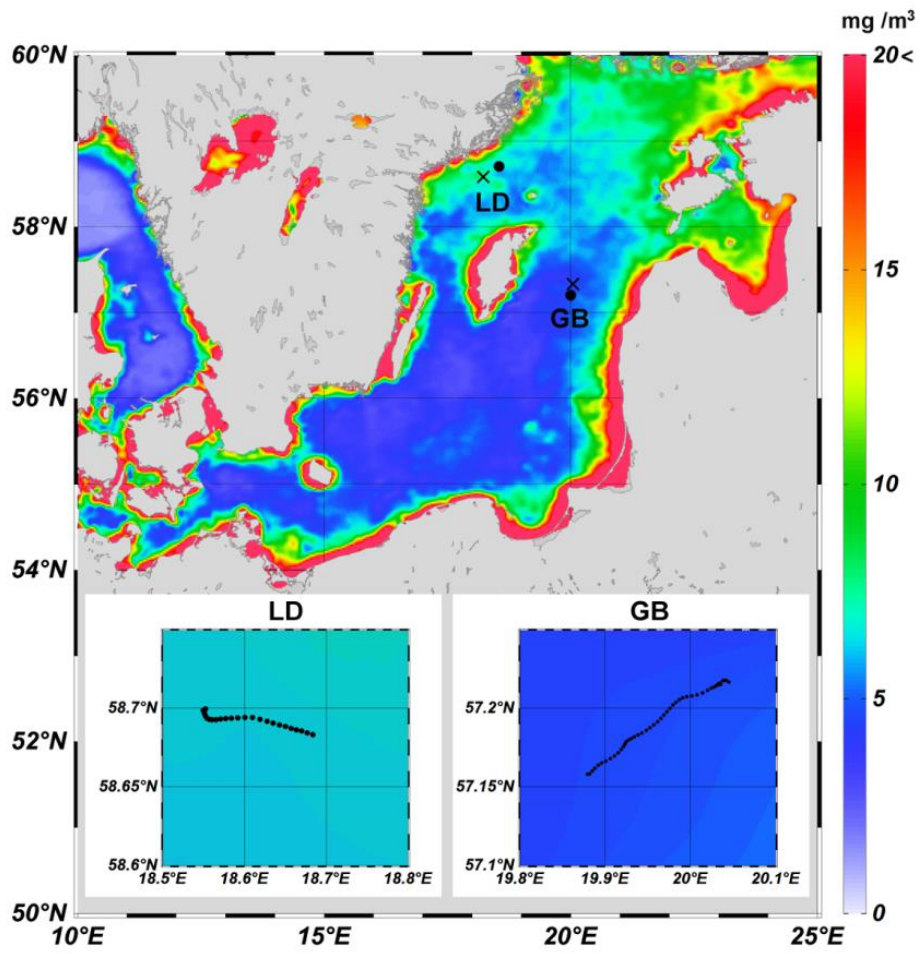


Fig. 1

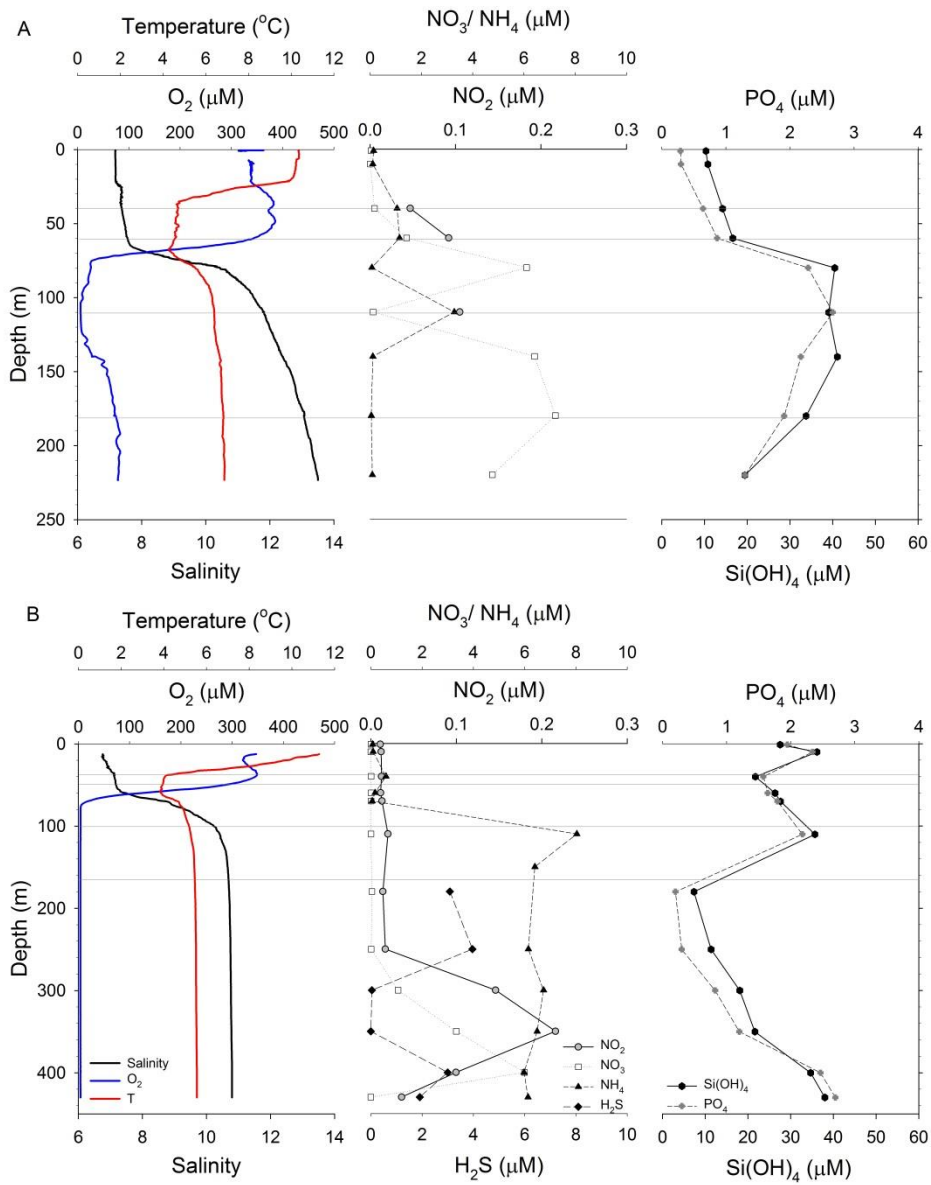


Fig. 2

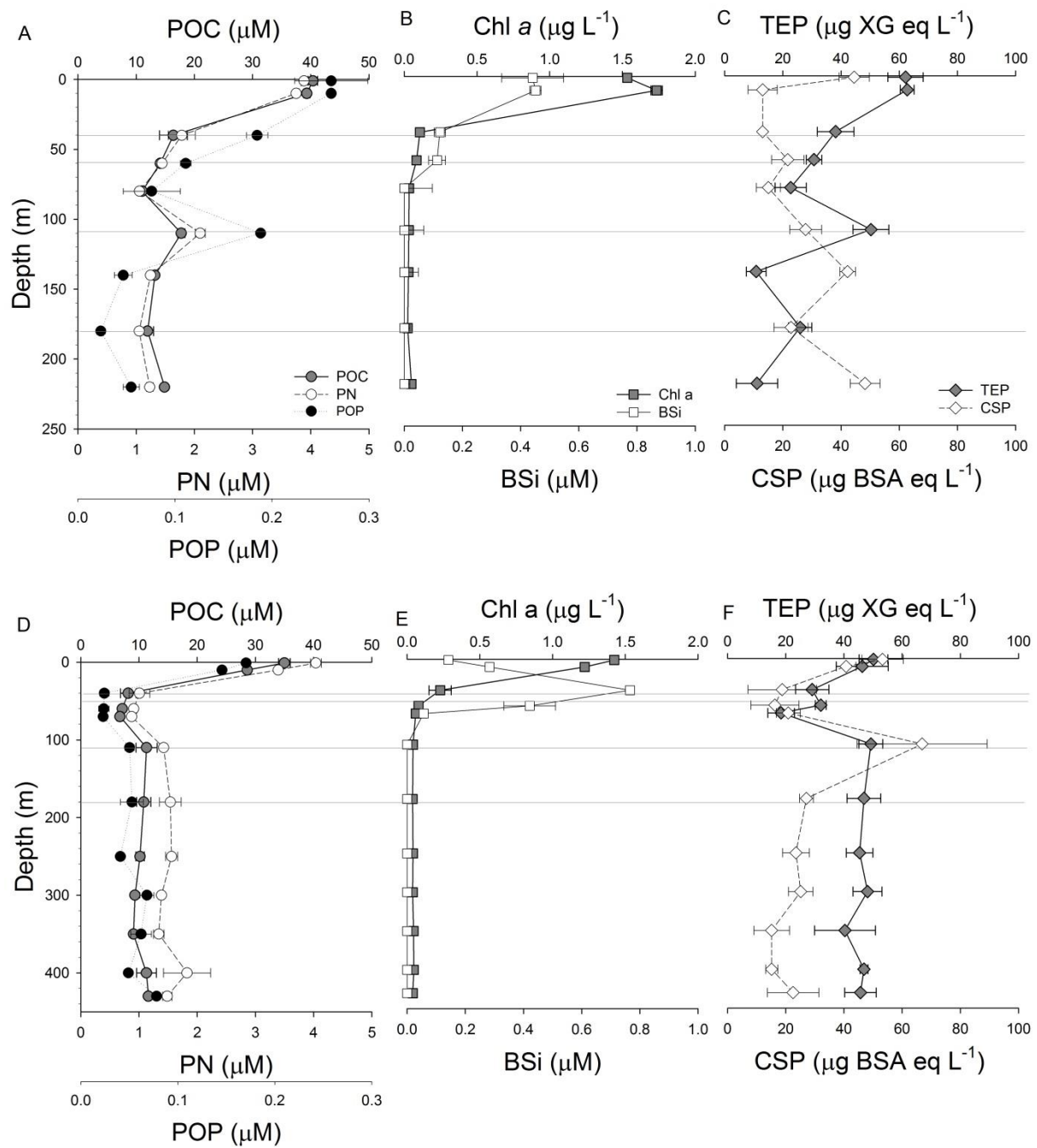


Fig. 3

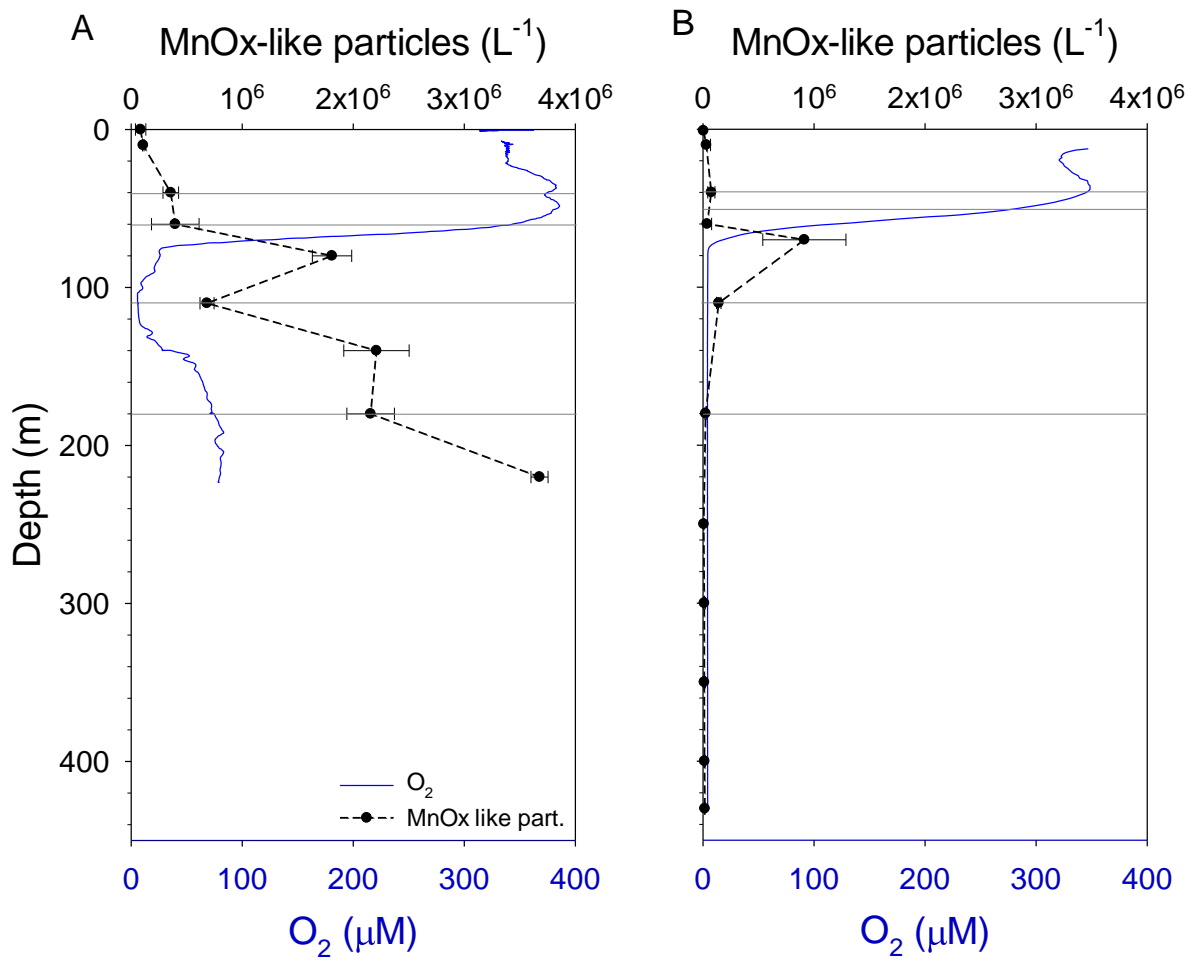


Fig. 4



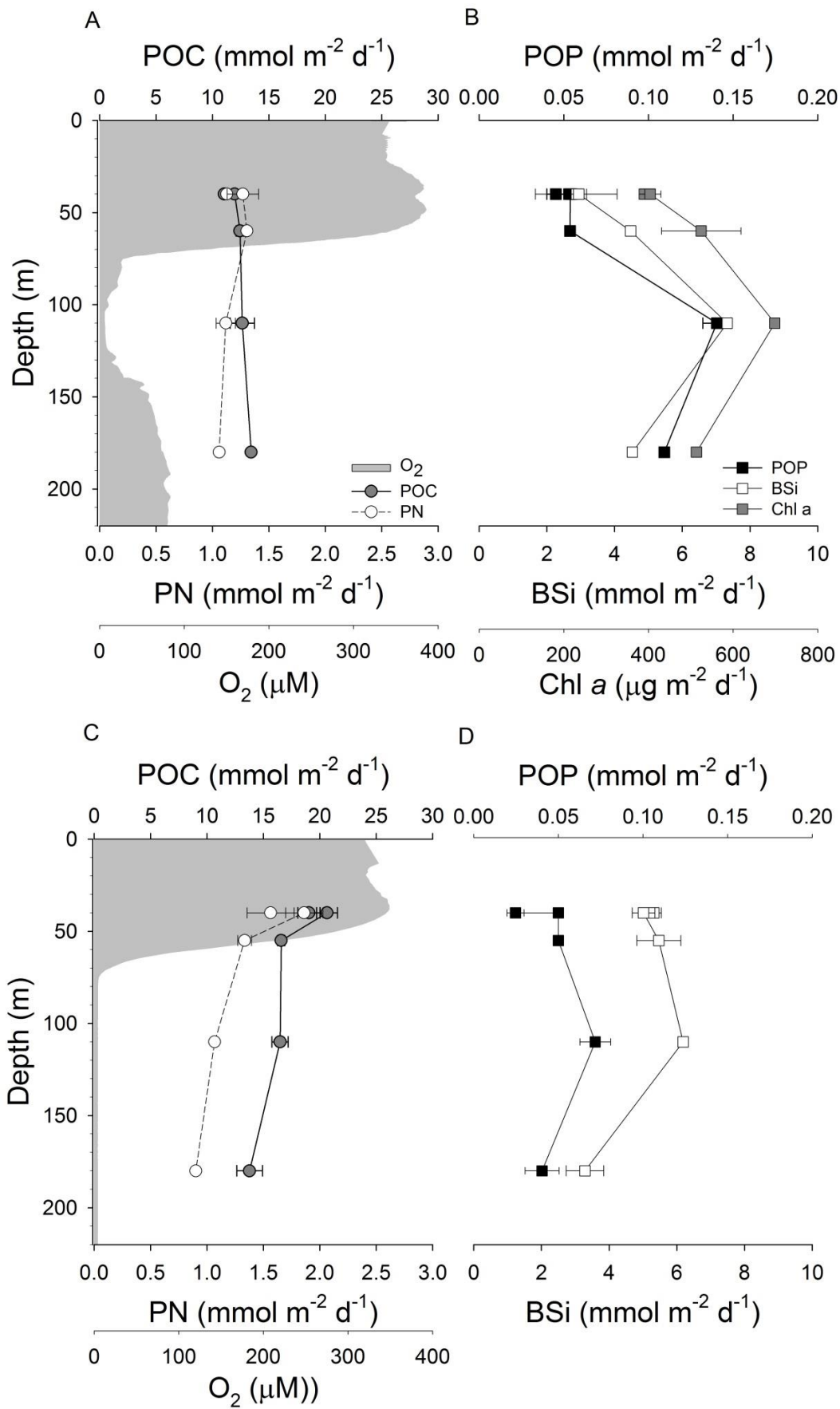


Fig. 5

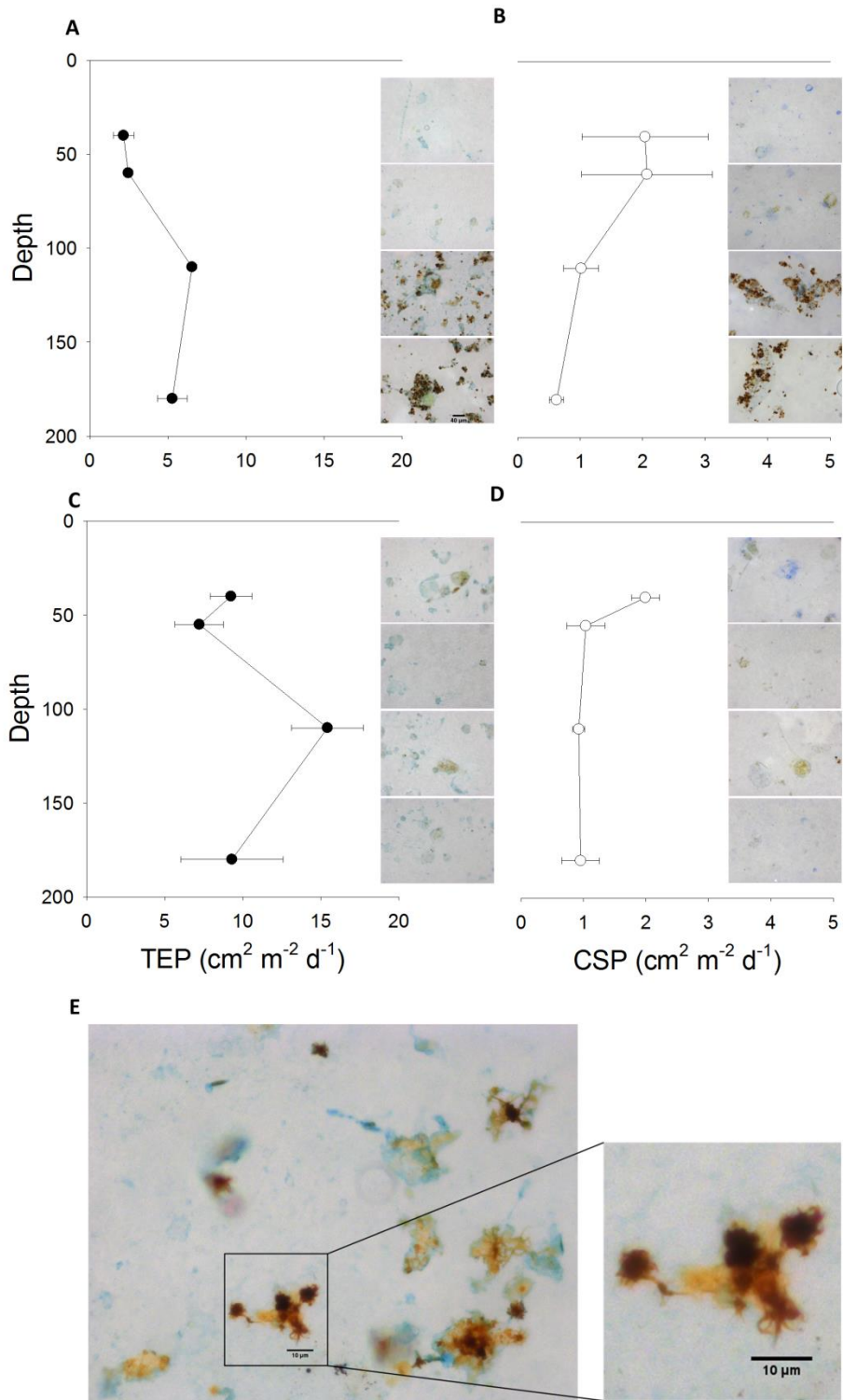


Fig. 6

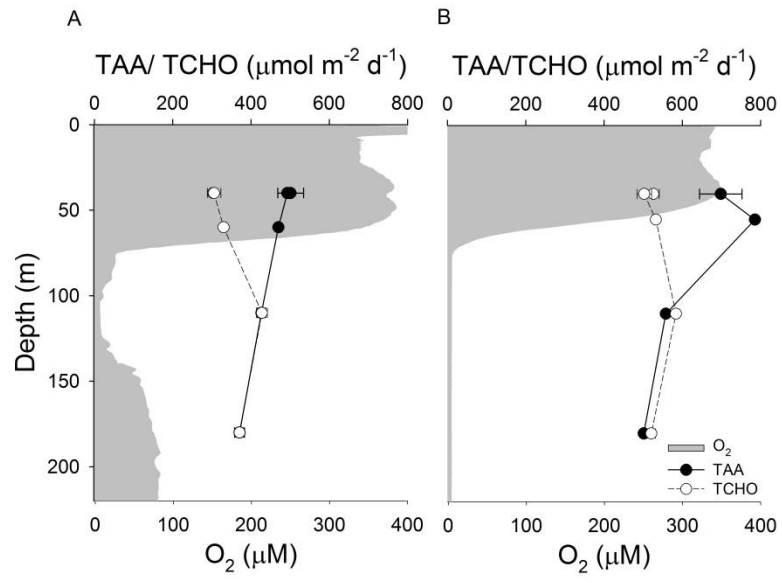


Fig. 7